Dynamic structure factor of vibrating fractals: Proteins as a case study

Shlomi Reuveni, Joseph Klafter, and Rony Granek

Dynamic Structure Factor of Vibrating Fractals: Proteins as a Case Study

Shlomi Reuveni,[1,2] Joseph Klafter,[1] and Rony Granek[3,*]

[1] *School of Chemistry, Tel-Aviv University, Tel-Aviv 69978, Israel*

[2] *Department of Statistics and Operations Research,*

School of Mathematical Sciences, Tel-Aviv University, Tel-Aviv 69978, Israel

[3] *The Stella and Avram Goren-Goldstein Department of Biotechnology Engineering,*

the Ilse Katz Institute for Meso and Nanoscale Science and Technology,

and the Reimund Stadler Minerva Center for Mesoscale Macromolecular Engineering,

Ben-Gurion University of The Negev, Beer Sheva 84105, Israel

* Corresponding author. E-mail: rgranek@bgu.ac.il

1

Abstract

We study the dynamic structure factor $S(k,t)$ of proteins at large wavenumbers k, $kR_g \gg 1$, where R_g is the gyration radius. At this regime measurements are sensitive to internal dynamics and we focus on vibrational dynamics of folded proteins. Exploiting the analogy between proteins and fractals, we perform a general analytic calculation of the displacement two-point correlation functions, $\langle (\vec{u}_i(t) - \vec{u}_j(0))^2 \rangle$. We confront the derived expressions with numerical evaluations that are based on protein data bank (PDB) structures and the Gaussian network model (GNM) for a few proteins and for the Sierpinski gasket as a controlled check. We use these calculations to evaluate $S(k,t)$ with arrested rotational and translational degrees of freedom, and show that the decay of $S(k,t)$ is dominated by the spatially averaged mean square displacement of an amino acid. The latter has been previously shown to evolve subdiffusively in time, $\langle (\vec{u}_i(t) - \vec{u}_i(0))^2 \rangle \sim t^\nu$, where ν is the anomalous diffusion exponent that depends on the spectral dimension d_s and fractal dimension d_f. As a result, for wavenumbers obeying $k^2 \langle \vec{u}^2 \rangle \gtrsim 1$, $S(k,t)$ effectively decays as a stretched exponential $S(k,t) \simeq S(k)e^{-(\Gamma_k t)^\beta}$ with $\beta \simeq \nu$, where the relaxation rate is $\Gamma_k \sim (k_B T/m\omega_o^2)^{1/\beta} k^{2/\beta}$, T is the temperature, and $m\omega_o^2$ the GNM effective spring constant describing the interaction between neighboring amino acids. The static structure factor is dominated by the fractal character of the native fold, $S(k) \sim k^{-d_f}$, with negligible to marginal influence of vibrations. The analytical expressions are first confronted with numerically based calculations on the Sierpinski gasket, and very good agreement is found between simulations and theory. We then perform PDB-GNM based numerical calculations for a few proteins, and an effective stretched exponential decay of the dynamic structure factor is found, albeit their relatively small size. However, when rotational and translational diffusion are added, we find that their contribution is never negligible due to finite size effects. While we can still attribute an effective stretching exponent β to the relaxation profile, this exponent is significantly larger than the anomalous diffusion exponent ν. We compare our theory with recent neutron spin-echo studies of myoglobin and hemoglobin, and conclude that experiments in which the rotational and translational degrees of freedom are arrested, e.g., by anchoring the proteins to a surface, will improve the detection of internal vibrational dynamics.

I. INTRODUCTION

In the last few years there has been renewed interest in the fractal-like nature of natively folded proteins [1–13]. In analogy with mathematically constructed fractals, it has been shown that each protein can be associated with characteristic broken dimensions. Diversity was understood in terms of the unique exponents that characterize each protein [3, 5, 8]. This viewpoint has allowed description of protein dynamics on a universal level and has led to a unified approach towards observed anomalies in the vibrational dynamics of proteins. On the experimental side, evidence of fractality in proteins came from electron spin relaxation measurements [11] and neutron scattering [12]. Indirect evidence came from single molecule experiments that have reported anomalous behaviors involving power-laws in time [14] and from molecular dynamics simulations that have shown anomalous diffusion of vibrational energy [3], dihedral angels [15] and amino acids [16]. These observations were further backed by various elastic network based studies [5–8, 10] concluding that anomalies in the vibrational dynamics of proteins are a consequence of a fractal-like structure [8]. Biological relevance of the fractal properties of proteins was discussed in Refs. [6–8, 13]. More recently, the fractal analysis has been proven useful to explain the action of antibodies [17].

Fractals are characterized by a few broken dimensions [18, 19]: (i) the mass fractal dimension d_f, that governs the scaling $M(r) \sim r^{d_f}$ of the mass $M(r)$ enclosed in concentric spheres of radius r, (ii) the spectral dimension d_s that governs the scaling $g(\omega) \sim \omega^{d_s-1}$ of the vibrational density of states (DOS) $g(\omega)$ with frequency ω [19–21], and (iii) the topological dimension d_l that governs the scaling $M(l) \sim l^{d_l}$ of the mass $M(l)$ enclosed in concentric "spheres" of radius l in the topological (or "manifold"/"chemical") space. One may also define, instead of d_l, the chemical length (or minimal path) dimension $d_{\min} = d_f/d_l$ that relates the real space distance r between two points on the fractal to the minimal path distance l between these points along the fractal network links, $l \sim r^{d_{\min}}$. The dimensions d_f and d_s have been computed for a large number of proteins using the native fold structures obtained from the protein data bank [7]. The fractal dimension d_f is computed from these structures in a straight forward manner. The topological dimension d_l has also been computed and found close to the fractal dimension d_f [22]. The computation of d_s requires a network elasticity model, and the Gaussian network model (GNM) has been mostly used [23]. The spectral dimension of the vast majority of proteins has been found to be smaller than two

[4, 6, 7]. Importantly, it leads to the generalized Landau-Peierls instability, $\langle u^2 \rangle \sim N^{\frac{2}{d_s}-1}$ where u is an amino acid displacement (averaged over all amino acids) and N is the number of amino acids [4, 6, 24]. By invoking marginal stability, that allows proteins to attain maximum fluctuations (or "flexibility") but keep their native fold structure, a universal equation of state that relates d_s, d_f and N, for all natively folded proteins [6], has been deduced. The equation has been validated for about 5,000 proteins and remarkable agreement has been found, regardless of protein source or function [7].

Recent advances in high-resolution inelastic neutron scattering, available with neutron spin-echo (NSE) spectroscopy, have turned this approach useful in the analysis of biomolecule flexibility and vibrational dynamics [25, 26]. NSE studies that measure the dynamic structure factor $S(k,t)$ have been recently performed on horse heart myoglobin and bovine hemoglobin in solutions [27]. In the large wavenumber k regime corresponding to $kR_g \gg 1$, where R_g is the gyration radius, and at low concentrations and times shorter than 1ns, the result is a stretched exponential relaxation, $S(k,t) \sim e^{-(\Gamma_k t)^\beta}$ with $\beta \simeq 0.4 \pm 0.03$ for both proteins and independent of k. The relaxation rate has been found to scale as $\Gamma_k \sim k^{2/\beta}$. Inelastic neutron scattering, a complementary method to NSE, is used for exploring protein dynamics at high frequencies ("short times") [28, 29]. Inelastic neutron scattering experiments and MD simulations performed on lysozyme showed a non-Lorentzian spectra which corresponds to a non-exponential decay with time of the dynamic structure factor [30]. These findings are in accord with the NSE findings described above and with the theory developed herein.

Phenomenologically, the non-exponential relaxation of $S(k,t)$ can be approached by assuming that collective/averaged observables, associated with the internal dynamics of proteins, follow fractional Brownian motion rather than regular Brownian motion [31, 32]. The assumption is justified a posteriori by comparison to MD simulations and experiments. Another approach towards the anomalous relaxation of $S(k,t)$ is based on an analogy with polymer dynamics theory and one conjectures that $S(k,t)$ decays mainly due to the time evolution of the amino acid mean square displacement (MSD) [33–35]. Combined with the above experimental observations, this conjecture suggests that the MSD evolves anomalously in time, i.e., as $\sim t^\nu$ with $\nu \simeq \beta$. Yet, the anomalous diffusion exponent does not fit any of the polymer theory exponents, 2/3 in the Zimm model and 1/2 in the Rouse model. More importantly, a folded protein is clearly nothing like a solvated, open, flexible polymer, that

fluctuates between its many available configurations without having any underlying scaffold. Hence, the use of polymer theory can only serve as a guiding tool.

In this paper we take a first principles approach and relate the anomalies in the decay of the dynamic structure factor with the fractal-like nature of proteins. We first note that on timescales less than or of order nanosecond a protein is not expected to experience any unfolding-refolding dynamics, even on a local scale, and all dynamics is expected to be associated with (overdamped) vibrations about the folded structure. Due to the protein fractal-like structure, the MSD of an amino acid, averaged over all amino acids of the protein, have been shown to be subdiffusive, that is to scale at short times as $\sim t^\nu$. The exponent ν depends on the fractal and spectral dimensions, $\nu = 1 - d_s/2$ in a Rouse type model [5, 8, 35], $\nu = (2 - d_s)/(2 - d_s + d_s/d_f)$ in a Zimm type model [10], and $\nu = 2 - d_s$ for vanishing friction [5]. Note that although we constantly use the polymer physics terms "Rouse" and "Zimm", these terms are only used in order to emphasize the hydrodynamic friction model in question. In a Rouse-type model the friction is local while in a Zimm-type model the friction is long ranged due to hydrodynamic interactions. In contrast to the original, polymeric, use of the terms "Rouse" and "Zimm", we obviously do not assume that a protein is modeled by a 1D Gaussian chain. On the contrary, as described later on, the native 3D structure is most definitely taken into consideration. Hence the anomalous diffusion exponents are in general different from their polymer values $\nu = 1/2$ (Rouse) and $\nu = 2/3$ (Zimm) [33]. Special fractals may yield the linear polymer Zimm exponent $\nu = 2/3$, e.g., the Vicsek fractals studied numerically by Blumen and co-workers [35] (as can also be verified by using the above analytic expression for ν), however, this is not typical. For further discussion about the difference between the Zimm-like and Rouse-like models used here, and those used in polymer theory, the reader is referred to Ref. [10].

Since all amino acids contribute to the dynamic structure factor, it should indeed exhibit the spatially averaged MSD. However, this single amino acid picture fails to capture both static and dynamic correlations between amino acids, e.g., it is unable to predict the static structure factor $S(k)$, and so this simplified viewpoint may not be complete. We thus make a complete calculation of the dynamic structure factor based on the fractal analogy, and delineate the regimes for which the decay of $S(k,t)$ is dominated by the MSD, thus connecting the fractal exponents d_s and d_f to the stretched exponential decay of $S(k,t)$. We also predict the dependence of the relaxation rate on the effective spring constant describing

5

the interaction between neighboring amino acids. Moreover, we add the non-trivial effect of rotational diffusion on the relaxation profile. In addition, we demonstrate the signature of protein fractal properties and fractal controlled vibrations on the static structure factor.

In order to obtain the dynamic structure factor, we calculate first the vibrational amino acid pair correlation function $\langle (u_i(t) - u_j(0))^2 \rangle$, which is a fundamental ingredient of the dynamic structure factor. We expand this correlation function in normal modes, obtain its scaling form, and relate it to two dynamical quantities that we have focussed on in the past: (i) the MSD of an amino acid, and (ii) the autocorrelation function of the distance between a pair of amino acids. We dwell on the different asymptotes of the pair correlation function that are relevant for the decay profile of the dynamic structure factor. We show that above a crossover time that signifies the passage of information (or energy [3]) between the two residues, the pair correlation function in question approaches the MSD. As the latter is subdiffusive, it leads to the stretched exponential decay of the dynamic structure factor.

II.   MODEL DEFINITIONS

We repeat briefly the model definitions and assumptions, following the notations of Ref. [5]. Protein vibrations are discussed using the Gaussian network model (GNM) [20, 23]. The model assigns identical springs between α-carbon pairs that are distant less than a cutoff distance R_c, whose typical values range between 6 to 8 A. Each α-carbon, henceforth named "bead", is assigned an averaged amino acid mass. In what follows, we assume that the network forms a disordered fractal. The index of a bead, or its coordinate in topological space, is denoted symbolically by the "vector" $\vec{l}$. The vector $\vec{R}(\vec{l})$ denotes its position in real space. (Note that this indexing method is equivalent to the indexing method used in the Abstract and Sec. I. In what follows we will use the two indexing methods interchangeably.) The ground configurational state of the protein is described by the set of coordinates $\vec{R}_{eq}(\vec{l})$, and deviations from the ground state are denoted by the displacements $\vec{u}(\vec{l}) = \vec{R}(\vec{l}) - \vec{R}_{eq}(\vec{l})$. The GNM Hamiltonian is

$$H\left[\{\vec{u}(\vec{l})\}\right] = \frac{1}{2}m\omega_o^2 \sum_{<\vec{l}\vec{l'}>} \left(\vec{u}(\vec{l}) - \vec{u}(\vec{l'})\right)^2 , \tag{1}$$

where $< \vec{l}\,\vec{l'} >$ stands for pairs connected by springs, ω_o is the spring self-frequency, and m is the bead mass ($m\omega_o^2$ is the spring constant). The eigenstates (normal modes) $\Psi_\alpha(\vec{l})$ of the

6

Hamitonian (1), are solutions of the eigenvalue equation

$$\omega_o^2 \sum_{\vec{l}' \in \vec{l}} [\Psi_\alpha(\vec{l}') - \Psi_\alpha(\vec{l})] = -\omega_\alpha^2 \Psi_\alpha(\vec{l}) \ , \tag{2}$$

where ω_α is the mode frequency. Here $\vec{l}' \in \vec{l}$ denotes beads connected by springs to the bead $\vec{l}$. $\{\Psi_\alpha(\vec{l})\}$ form an orthonormal set [19, 21] such that

$$\sum_{\vec{l}} \Psi_\alpha(\vec{l}) \Psi_\beta(\vec{l}) = \delta_{\alpha,\beta} \tag{3}$$

and

$$\sum_\alpha \Psi_\alpha(\vec{l}) \Psi_\alpha(\vec{l}') = \delta_{\vec{l},\vec{l}'} \ . \tag{4}$$

This allows to define a normal mode transform

$$\vec{u}_\alpha = \sum_{\vec{l}} \vec{u}(\vec{l}) \Psi_\alpha(\vec{l}) \ , \tag{5}$$

and an inverse transform

$$\vec{u}(\vec{l}) = \sum_\alpha \vec{u}_\alpha \Psi_\alpha(\vec{l}) \ , \tag{6}$$

where $\vec{u}_\alpha$ is the amplitude of the normal mode $\Psi_\alpha(\vec{l})$. In the normal mode "space", the Hamiltonian is diagonal,

$$H\left[\{\vec{u}_\alpha\}\right] = \frac{1}{2} m \sum_\alpha \omega_\alpha^2 \vec{u}_\alpha^2 \ . \tag{7}$$

Equipartition theorem then dictates that at thermal equilibrium

$$\langle \vec{u}_\alpha \cdot \vec{u}_\beta \rangle_T = \frac{3 k_B T}{m \omega_\alpha^2} \delta_{\alpha,\beta} \ . \tag{8}$$

On a fractal, the normal modes $\Psi_\alpha(\vec{l})$ are strongly localized in space, unlike the oscillatory behavior characteristic of uniform networks. A disorder averaged eigenstate may be defined according to

$$\bar{\Psi}(\omega_\alpha, |\vec{\ell} - \vec{\ell}'|) = N \langle \Psi_\alpha(\vec{\ell}) \Psi_\alpha(\vec{\ell}') \rangle_{\text{dis}} \ , \tag{9}$$

where $\langle ... \rangle_{\text{dis}}$ denotes disorder averaging, i.e. averaging over all realizations of the fractal keeping the nodes $\vec{\ell}$ and $\vec{\ell}'$ fixed, or averaging, within a given realization, over all different pair of nodes $\vec{\ell}$ and $\vec{\ell}'$ that have the same topological space distance $|\vec{\ell} - \vec{\ell}'|$. Note that mode normalization implies $\langle \Psi_\alpha(\vec{\ell})^2 \rangle_{\text{dis}} = 1/N$. It has been shown that $\bar{\Psi}(\omega_\alpha, l)$ obeys the following scaling form [18, 20, 21]

$$\bar{\Psi}(\omega_\alpha, l) = f\left[(\omega_\alpha/\omega_o)^{d_s/d_l} l \right] \ , \tag{10}$$

where $f(y)$ is the scaling function. For $y \gg 1$, $f(y)$ is *exponentially decaying*, and, for $y \ll 1$, $f(y) \simeq 1 - C_0 \times y^2$ where C_0 is a numerical constant [21, 36, 37].

III. TWO-POINT CORRELATION FUNCTION AND MEAN SQUARE DISPLACEMENT

A. Introduction

In order to derive the dynamic structure factor of proteins at large wavenumbers and short times, we discuss first the relevant displacement pair correlation functions that are needed for this calculation. We are specifically interested in the pair correlation function $\langle (\vec{u}(\vec{\ell},t) - \vec{u}(\vec{\ell'},0))^2 \rangle$, where it is understood that spatial averaging, i.e. averaging over many origins $\vec{\ell'}$ that are sufficiently far from the periphery, has been performed, thus making this correlation function depend only on the relative separation $|\vec{\ell} - \vec{\ell'}|$ in topological space. In particular, for $\vec{\ell} = \vec{\ell'}$, this correlation function reduces simply to the (spatially averaged) MSD of an amino acid.

B. Basic dynamics

In Refs. [5, 8, 10] we derived the normal mode space Langevin equations for the fractal-like protein in the high damping and vanishing damping limits. In the high damping limit, which is our main focus here due to its relevance to protein dynamics in solutions, two models were considered: (i) a Rouse type model in which the hydrodynamic friction is local, and (ii) a Zimm type model where we accounted for the hydrodynamic interaction between different amino acids, that is transmitted through the velocity field of the solvent. For both models, the Langevin equations of motion in the mode space can be written in the form

$$\frac{d\vec{u}_\alpha}{dt} = -\Gamma_\alpha \vec{u}_\alpha + \vec{\zeta}_\alpha(t) . \tag{11}$$

where $u_\alpha(t)$ is the amplitude of a normal mode α at time t,

$$\Gamma_\alpha = m\omega_\alpha^2 \Lambda_\alpha \tag{12}$$

is the mode relaxation rate, $\vec{\zeta}_\alpha(t)$ is thermal white noise that obeys the fluctuation-dissipation theorem

$$\langle \vec{\zeta}_\alpha(t)\vec{\zeta}_\beta(t') \rangle = 2k_B T \Lambda_\alpha \delta_{\alpha,\beta} \delta(t - t') , \tag{13}$$

and Λ_α is the mode mobility coefficient. Using Eq. (11), the time autocorrelation function of a mode amplitude obeys a simple exponential decay controlled by Γ_α,

$$\langle \vec{u}_\alpha(t) \cdot \vec{u}_\alpha(0) \rangle = \langle \vec{u}_\alpha^{\,2} \rangle_T e^{-\Gamma_\alpha t} . \tag{14}$$

The dependence of Λ_α on ω_α is sensitive to the hydrodynamic model in question. In the Rouse model

$$\Lambda_\alpha = 1/m\gamma \tag{15}$$

independent of frequency, where $m\gamma$ is the friction coefficient of a bead. Thus $m\gamma \simeq 3\pi\eta b$ for Stokes friction, where b is the bead diameter, taken for simplicity equal to the mean bond length $(b \leq R_c)$. In the Zimm model,

$$\Lambda_\alpha = (A/6\pi\eta b) \, (\omega_\alpha/\omega_o)^{\frac{d_s}{d_f} - d_s} , \tag{16}$$

where A is a numerical constant,

$$A = \frac{d_l \pi^{d_l/2}}{\Gamma[d_l/2 + 1]} \int_0^\infty dx \; x^{d_l - 1 - d_l/d_f} f(x) . \tag{17}$$

($f(x)$ is the mode scaling function defined in Eq. (10).)

To account for both models in a single formula, we shall write the relaxation rate as

$$\Gamma_\alpha \simeq \bar{A} \, \omega_\alpha^{\,\theta} \tag{18}$$

where (i) in the Rouse model:

$$\theta = 2 ; \quad \bar{A} = 1/\gamma = m/(3\pi\eta b) , \tag{19}$$

and (ii) in the Zimm model:

$$\theta = 2 - d_s + d_s/d_f ; \quad \bar{A} = A \, m/(6\pi\eta b\omega_o^{\frac{d_s}{d_f} - d_s}) . \tag{20}$$

C.   Two-point correlation function: Basic expressions

Expanding the two point correlation function in terms of the exact normal modes $\Psi_\alpha(\vec{\ell})$ we find

$$\langle (\vec{u}(\vec{\ell}, t) - \vec{u}(\vec{\ell'}, 0))^2 \rangle =$$
$$\sum_\alpha \langle \vec{u}_\alpha^{\,2} \rangle_T \left(\Psi_\alpha(\vec{\ell})^2 + \Psi_\alpha(\vec{\ell'})^2 - 2\Psi_\alpha(\vec{\ell})\Psi_\alpha(\vec{\ell'})e^{-\Gamma_\alpha t} \right) .$$
$$\tag{21}$$

9

Performing disorder average over Eq. (21) (see definition after Eq. (9)), and using the definition of the disorder averaged normal mode $\bar{\Psi}(\omega_\alpha, \ell)$, Eq. (9), the two-point correlation function which we focus on is found to be

$$\langle (\vec{u}(\vec{\ell}, t) - \vec{u}(\vec{\ell'}, 0))^2 \rangle =$$
$$\frac{2}{N} \sum_\alpha \langle \vec{u}_\alpha^2 \rangle_T \left(1 - \bar{\Psi}(\omega_\alpha, |\vec{\ell} - \vec{\ell'}|) e^{-\Gamma_\alpha t} \right) . \tag{22}$$

If the fractal (protein) is sufficiently large, the frequency spectrum is dense and we can approximate the sum by an integral over the frequency ω using the DOS $g(\omega) = n_o \omega^{d_s - 1}$, where $n_o = N d_s / \omega_o^{d_s}$ is chosen such that $\int_0^{\omega_o} d\omega g(\omega) = N$. Making use of the equipartition theorem, Eq. (8), we obtain

$$\langle (\vec{u}(\vec{\ell}, t) - \vec{u}(\vec{\ell'}, 0))^2 \rangle = 6 d_s \frac{k_B T}{m \omega_o^{d_s}} \int_{\omega_{\min}}^{\omega_o} d\omega \, \omega^{d_s - 3} \times$$
$$\left(1 - \bar{\Psi}(\omega, |\vec{\ell} - \vec{\ell'}|) e^{-\bar{A} \omega^\theta t} \right) . \tag{23}$$

Note that the lower and upper integration limits in Eq. (23) set the shortest and longest vibrational relaxation times in the system. The longest relaxation time τ_N is the inverse of the smallest relaxation rate leading to $\tau_N = \Gamma(\omega_{\min})^{-1} \simeq \bar{A}^{-1} \omega_{\min}^{-\theta}$ where $\omega_{\min} \simeq \omega_o (R_g/b)^{-d_f/d_s}$, i.e.

$$\tau_N \simeq \bar{A}^{-1} \omega_o^{-\theta} (R_g/b)^{\theta d_f/d_s} \sim N^{\theta/d_s} ; . \tag{24}$$

The shortest relaxation time τ_0 is is the inverse of the largest relaxation rate thereby

$$\tau_0 = \Gamma(\omega_o)^{-1} = \bar{A}^{-1} \omega_o^{-\theta} . \tag{25}$$

Focusing on the intermediate time regime $\tau_0 \ll t \ll \tau_N$ we may set the lower and upper limits of integration in Eq. (23) to 0 and infinity, respectively. Changing the variable of integration from ω to z, where $z^\theta = \bar{A} \omega^\theta t$, and using the scaling form of the eigenstates, $\bar{\Psi}(\omega, l) = f\left[(\omega_\alpha/\omega_o)^{d_s/d_l} l \right]$, we obtain the following scaling form

$$\langle (\vec{u}(\vec{\ell}, t) - \vec{u}(\vec{\ell'}, 0))^2 \rangle = \frac{k_B T}{m \omega_o^{d_s}} (\bar{A} t)^\nu \, \Phi \left[|\vec{\ell} - \vec{\ell'}| / \ell(t) \right] , \tag{26}$$

where

$$\Phi(v) = 6 d_s \int_0^\infty dz z^{d_s - 3} \left(1 - f\left[z^{d_s/d_l} v \right] e^{-z^\theta} \right) \tag{27}$$

and where $\ell(t) = \omega_o^{d_s/d_l} (\bar{A} t)^{\frac{d_s}{d_l \theta}}$ is the (dimensionless) length describing the propagation with distance, in topological space, of the bead-bead correlations or force/enregy perturbations.

10

In real space, this (dimensioned) propagation length is

$$\xi(t) \simeq b\ell(t)^{d_l/d_f} = b\,\omega_o^{d_s/d_f}\,\bar{A}^\zeta\,t^\zeta \tag{28}$$

where

$$\zeta = \frac{d_s}{d_f\theta} \tag{29}$$

is the real space propagation length exponent. We note that in the Rouse model $\zeta = 1/d_w$, where d_w, the random walk (RW) anomalous diffusion exponent, is given by the Alexander-Orbach relation [20]

$$d_w = \frac{2d_f}{d_s} \tag{30}$$

(i.e. $\langle r^2(t)\rangle \sim t^{2/d_w}$ for random walk on the same network).

Molecular dynamics simulations aimed at characterizing the spread of vibrational energy in proteins [3] and random walk simulations on proteins [8] have confirmed the power law behavior of the propagation length both directly and indirectly. In particular, it was found that in proteins $d_w > 2$, i.e., propagation of correlations and force/energy perturbations in the Rouse model is subdiffusive in time.

D. Mean square displacement

In particular, for $\vec{\ell} = \vec{\ell'}$ we recover the previously derived vibrational MSD of a bead, averaged over all network beads. Provided that $d_s < 2$, it shows the familiar *anomalous subdiffusion*

$$\langle \Delta\vec{u}(t)^2\rangle \equiv \langle(\vec{u}(\vec{\ell},t) - \vec{u}(\vec{\ell},0))^2\rangle = B\,t^\nu\;. \tag{31}$$

The exponent ν is

$$\nu = (2 - d_s)/\theta \tag{32}$$

yielding

$$\nu = 1 - \frac{d_s}{2} \tag{33}$$

in the Rouse model, and

$$\nu = \frac{2 - d_s}{2 - d_s + d_s/d_f} = \frac{d_w - d_f}{d_w - d_f + 1} \tag{34}$$

in the Zimm model. The prefactor B is

$$B = \Phi[0]\frac{k_B T}{m\omega_o^{d_s}}\bar{A}^\nu\;. \tag{35}$$

Using $f(0) = 1$ and performing the integration in Eq. (27), we find (i) $\Phi[0] = \frac{6d_s\Gamma[\frac{d_s}{2}]}{2-d_s}$ in the Rouse model, and (ii) $\Phi[0] = \frac{6d_s\Gamma[\frac{1}{d_w-d_f+1}]}{2-d_s}$ in the Zimm model ($\Gamma[x]$ is the Gamma function). Importantly, we have verified Eq. (31) for about 500 proteins by calculating its RW counterpart, the probability of return to the origin, which is exactly proportional to the time derivative of the Rouse model vibrational MSD [8].

The anomalous subdiffusion is expected to hold for times $\tau_0 \ll t \ll \tau_N$. For $t \gtrsim \tau_N$ the MSD saturates at $\langle\Delta\vec{u}(\infty)^2\rangle = 2\langle\vec{u}^2\rangle$, i.e. it is proportional to the so-called (mean) B-factors. As previously shown, the latter exhibits the generalized Landau-Peierls instability $\langle\vec{u}^2\rangle \sim N^{2/d_s-1}$. The Landau-Peierls instability may be deduced from the integral expression

$$\langle\vec{u}^2\rangle = 6d_s\frac{k_BT}{m\omega_o^{d_s}}\int_{\omega_{\min}}^{\omega_o} d\omega \, \omega^{d_s-3} \tag{36}$$

that for $d_s < 2$ diverges at the lower limit $\omega_{\min}$,

$$\langle\vec{u}^2\rangle \simeq \frac{6d_s}{2-d_s}\frac{k_BT}{m\omega_o^{d_s}}\omega_{\min}^{d_s-2} \simeq \frac{6d_s}{2-d_s}\frac{k_BT}{m\omega_o^2}\left(\frac{R_g}{b}\right)^{d_w-d_f} \sim N^{2/d_s-1} \, . \tag{37}$$

Interestingly, for $\tau_0 \ll t$ the MSD may be shown to obey a simple scaling formula that includes the crossover to saturation

$$\langle\Delta\vec{u}(t)^2\rangle = \langle\vec{u}^2\rangle\phi\,[t/\tau_N] \, . \tag{38}$$

Note that the anomalous diffusion exponent $\nu = (2-d_s)/\theta$ can be deduced solely from the demand that, for $t \ll \tau_N$, the MSD should not depend on N. Thus $\phi[z] \sim z^{(2-d_s)/\theta}$ for $z \ll 1$, and $\phi[z] \to 2$ for $z \to \infty$.

E. Autocorrelation of distance

A closely related correlation function is the autocorrelation function $\langle\vec{x}(t)\cdot\vec{x}(0)\rangle$ of the fluctuations $\vec{x}(t)$ in the vector of separation between two points, where $\vec{x}(t)$ can be related to the displacements by $\vec{x}(t) = \vec{u}(\vec{\ell},t) - \vec{u}(\vec{\ell'},t)$. Note that $\langle\vec{x}(t)\cdot\vec{x}(0)\rangle$ is *not* identical to $\langle(\vec{u}(\vec{\ell},t) - \vec{u}(\vec{\ell'},0))^2\rangle$. However, under disorder averaging we can exactly write the two-particle correlation function in question as the sum of the single particle MSD and the distance autocorrelation function (see Appendix A.1),

$$\langle(\vec{u}(\vec{\ell},t) - \vec{u}(\vec{\ell'},0))^2\rangle = \langle\Delta\vec{u}(t)^2\rangle + \langle\vec{x}(t)\cdot\vec{x}(0)\rangle \tag{39}$$

(A similar expression holds without disorder averaging, see Appendix A.2.)

$\langle \vec{x}(t) \cdot \vec{x}(0) \rangle$ has been previously analyzed in great detail for short and long times. In particular, for $d_s < 2$ the static variance $\langle \vec{x}^{\,2} \rangle$ has been shown to diverge with distance as [5, 8, 38] $\langle \vec{x}^{\,2} \rangle \sim R_{ll'}^{d_w - d_f}$, where

$$R_{ll'} \equiv |\vec{R}_\ell - \vec{R}_{\ell'}| \tag{40}$$

is the Euclidean distance between beads $\vec{\ell}$ and $\vec{\ell'}$. This demonstrates the divergence with distance of the inter-particle separation fluctuations (in accord with the Landau-Peierls instability), as recently verified numerically for about 500 proteins [8]. More precisely, putting $t = 0$ in Eqs. (39) and (23) we find, provided that $d_s < 2$ and $2\frac{d_s}{d_l} + d_s > 2$ (assuming $f(y) \simeq 1 - C_0 y^2$ for $y \ll 1$),

$$\begin{aligned}
\langle \vec{x}^{\,2} \rangle &= 6 d_s \frac{k_B T}{m \omega_o^{d_s}} \times \int_0^\infty d\omega \, \omega^{d_s - 3} \left(1 - f \left[(\omega/\omega_o)^{d_s/d_l} l \right] \right) \\
&\simeq C \frac{k_B T}{m \omega_o^2} \left(\frac{R_{ll'}}{b} \right)^{d_w - d_f}
\end{aligned} \tag{41}$$

where $C = 6 d_s \int_0^\infty dz \, z^{d_s - 3} \left(1 - f(z^{d_s/d_l}) \right)$. Note that the static variance may be described by an effective harmonic potential $\frac{1}{2} m \omega_{\text{eff}}^2 \vec{x}^{\,2}$ with [21] $\omega_{\text{eff}}^2 \approx \omega_o^2 (R_{ll'}/b)^{d_f - d_w}$. Importantly, it has been proven proportional to the RW mean first passage time between $\vec{\ell}$ and $\vec{\ell'}$ on the same network, a fact that has far reaching consequences [8, 38, 39]. For $d_s \geq 2$ a different behavior is obtained that is rarely relevant to proteins and is therefore not discussed here [8, 38, 39].

We repeat briefly the asymptotic analysis of $\langle \vec{x}(t) \cdot \vec{x}(0) \rangle$ for short and long times. From Eqs. (39) and (23) we find

$$\begin{aligned}
\langle \vec{x}(t) \cdot \vec{x}(0) \rangle = 6 d_s \frac{k_B T}{m \omega_o^{d_s}} \int_{\omega_{\min}}^{\omega_o} d\omega \, \omega^{d_s - 3} \times \\
\left(1 - \bar{\Psi}(\omega_\alpha, |\vec{\ell} - \vec{\ell'}|) \right) e^{-\bar{A} \omega^\theta t} ,
\end{aligned} \tag{42}$$

which may be expressed in the following scaling form

$$\langle \vec{x}(t) \cdot \vec{x}(0) \rangle = \frac{k_B T}{m \omega_o^{d_s}} (\bar{A} t)^\nu \, \Omega \left[|\vec{\ell} - \vec{\ell'}|/\ell(t) \right] , \tag{43}$$

where

$$\Omega[v] = 6 d_s \int_0^\infty dz \, z^{d_s - 3} \left(1 - f \left[z^{d_s/d_l} v \right] \right) e^{-z^\theta} . \tag{44}$$

Note the subtle, yet fundamental, difference between Eqs. (43)-(44) and Eqs. (26)-(27).

If $\ell(t) \ll |\vec{\ell} - \vec{\ell'}|$ (short times), the two beads' motion is uncorrelated, and (see Sec. III.D) each bead performs anomalous subdiffusion. To find the asymptote in this limit we add and subtract 1 to the integrand in Eq. (42) to obtain

$$
\begin{aligned}
\langle \vec{x}(t) \cdot \vec{x}(0) \rangle = {} & \\
6 d_s \frac{k_B T}{m \omega_o^{d_s}} & \int_{\omega_{\min}}^{\omega_o} d\omega \, \omega^{d_s - 3} \left(1 - \bar{\Psi}(\omega_\alpha, |\vec{\ell} - \vec{\ell'}|) \right) \\
- 6 d_s \frac{k_B T}{m \omega_o^{d_s}} & \int_{\omega_{\min}}^{\omega_o} d\omega \, \omega^{d_s - 3} \left(1 - \bar{\Psi}(\omega_\alpha, |\vec{\ell} - \vec{\ell'}|) \right) \times \\
& \left(1 - \mathrm{e}^{-\bar{A} \omega^\theta t} \right) .
\end{aligned}
\tag{45}
$$

We can then neglect $\bar{\Psi}(\omega_\alpha, |\vec{\ell} - \vec{\ell'}|)$ in the second integral in Eq. (45), consistent with $\ell(t) \ll |\vec{\ell} - \vec{\ell'}|$ and exponentially decaying normal modes (see discussion after Eq. (10)). This can be easily understood by changing the integration variable of the second integral to $z = \omega(\bar{A}t)^{1/\theta}$, and use $f\left[z^{d_s/d_l} |\vec{\ell} - \vec{\ell'}| / \ell(t) \right] \ll 1$ for non-vanishing z (since for vanishing z the contribution to the integral is negligible). The second integral then becomes identical to the MSD. Provided that $d_s < 2$, at short times we thus find

$$
\langle \vec{x}(t) \cdot \vec{x}(0) \rangle \approx \langle \vec{x}^{\,2} \rangle - B t^\nu
\tag{46}
$$

where B is given by Eq. (35).

At long times such that $\ell(t) \gg |\vec{\ell} - \vec{\ell'}|$ the motion of the two particles is highly correlated, which leads to a vanishing autocorrelation of $\vec{x}(t)$. Using $f(y) \simeq 1 - C_0 \times y^2$ for $y \ll 1$ (C_0 is of order 1), we find, provided that $2 < 2\frac{d_s}{d_l} + d_s$,

$$
\langle \vec{x}(t) \cdot \vec{x}(0) \rangle \simeq C_1 \frac{k_B T}{m \omega_o^{d_s(1 + 2/d_l)}} \left(\frac{R_{ll'}}{b} \right)^{2 d_f / d_l} (\bar{A} t)^{-\mu}
\tag{47}
$$

where $\mu = 2 d_s / (d_l \theta) - \nu$, thereby

$$
\mu = \frac{d_s}{d_l} + d_s / 2 - 1
\tag{48}
$$

in the Rouse model, and

$$
\mu = \frac{2 \frac{d_s}{d_l} + d_s - 2}{2 - d_s + d_s / d_f} = \frac{2 \frac{d_f}{d_l} + d_f - d_w}{d_w - d_f + 1}
\tag{49}
$$

in the Zimm model. The numerical prefactor C_1 is $C_1 = 6 d_s C_0 \Gamma[(d_s(1 + 2/d_l) - 2)/\theta]/\theta$.

To summarize the time dependencies, we find

$$\langle \vec{x}(t) \cdot \vec{x}(0) \rangle \sim \begin{cases} 1 - \text{const.} \times t^\nu & \text{for } t \ll t^*(R_{ll'}) \\ t^{-\mu} & \text{for } t \gg t^*(R_{ll'}), \end{cases} \tag{50}$$

where

$$t^*(r) = \bar{A}^{-1} \omega_o^{-\theta} \left(\frac{r}{b} \right)^{d_f \theta / d_s} . \tag{51}$$

Thus $t^*(r) \sim r^{d_f \theta / d_s}$ and, in particular, $t^*(r) \sim r^{d_w}$ for the Rouse model.

F. Two-point correlation function: Scaling expressions

Combing the asymptotic results for $\langle \vec{x}(t) \cdot \vec{x}(0) \rangle$ with $\langle \Delta \vec{u}(t)^2 \rangle$ we obtain the following asymptotic behavior of the two-point correlation function under study. For short times, $t \ll t^*(R_{ll'})$, the correlation function is very close to its static value

$$\langle (\vec{u}(\vec{\ell}, t) - \vec{u}(\vec{\ell'}, 0))^2 \rangle \simeq C \frac{k_B T}{m \omega_o^2} \left(\frac{R_{ll'}}{b} \right)^{d_w - d_f} . \tag{52}$$

Corrections to this result are of higher order than those discussed here. A crossover to a subdiffusive behavior occurs at $t \sim t^*(R_{ll'})$, and for long times, $t^*(R_{ll'}) \ll t \ll \tau_N$, we find

$$\langle (\vec{u}(\vec{\ell}, t) - \vec{u}(\vec{\ell'}, 0))^2 \rangle \simeq B \, t^\nu \, + \\ C_1 \frac{k_B T}{m \omega_o^{d_s(1 + 2/d_l)}} \left(\frac{R_{ll'}}{b} \right)^{2 d_f / d_l} (\bar{A} t)^{-\mu} . \tag{53}$$

The second term in Eq. (53) is a small correction to the dominant time behavior $\langle (\vec{u}(\vec{\ell}, t) - \vec{u}(\vec{\ell'}, 0))^2 \rangle \sim t^\nu$ that is independent of $R_{ll'}$.

To end this discussion, note that all scaling properties described in this section can be transformed from topological space to the real 3D Euclidean space. Thus the two-point correlation function, Eq. (26), can be rewritten as

$$\langle (\vec{u}(\vec{\ell}, t) - \vec{u}(\vec{\ell'}, 0))^2 \rangle = \frac{k_B T}{m \omega_o^{d_s}} (\bar{A} t)^\nu \, \Phi_1 \left[\frac{R_{ll'}}{\xi(t)} \right] , \tag{54}$$

where $\Phi_1[u] = \Phi[u^{d_f/d_l}]$. $\Phi_1[u]$ has the following asymptotes: (i) $\Phi_1[u] \simeq \text{const.}$ for $u \ll 1$ (to leading order), or, more precisely, $\Phi_1[u] \simeq \Phi[0] + \text{const.} \times u^{2 d_f / d_l}$ (where the second term is negligible); and (ii) $\Phi_1[u] \sim u^{d_w - d_f}$ for $u \gg 1$. Other equivalent expressions are

$$\langle (\vec{u}(\vec{\ell}, t) - \vec{u}(\vec{\ell'}, 0))^2 \rangle = \frac{k_B T}{m \omega_o^{d_s}} (\bar{A} t)^\nu \, \Phi_2 \left[\frac{t}{t^*(R_{ll'})} \right] , \tag{55}$$

15

where $\Phi_2[u] = \Phi[u^{-d_s/(d_l\theta)}]$, and

$$\langle(\vec{u}(\vec{\ell},t) - \vec{u}(\vec{\ell}',0))^2\rangle = \frac{k_B T}{m\omega_o^2}\left(\frac{R_{ll'}}{b}\right)^{d_w-d_f} \Phi_3\left[\frac{t}{t^*(R_{ll'})}\right], \tag{56}$$

where $\Phi_3[u] = u^\nu\Phi[u^{-d_s/(d_l\theta)}]$. $\Phi_3[u]$ has the following asymptotes: (i) $\Phi_3[u] \simeq$ const. for $u \ll 1$, and (ii) $\Phi_3[u] \sim u^\nu$ for $u \gg 1$ (to leading order), or, more precisely, $\Phi_3[u] \simeq \Phi[0]u^\nu + \text{const.}u^{-\mu}$ (where the second term is negligible). Eq. (56) is particularly useful for the numerical analysis that we perform next.

G. Numerical results for the Sierpinski gasket and proteins

1. Sierpinski gasket

To test the above analytic expression we first evaluate numerically the pair correlation function $\langle(\vec{u}(\vec{\ell},t) - \vec{u}(\vec{\ell}',0))^2\rangle$ on a vibrating Sierpinski gasket [18, 20] (fractal and spectral dimensions: $d_f = \ln(3)/\ln(2) \simeq 1.585, d_s = 2\ln(3)/\ln(5) \simeq 1.3652$) having $N = 6561$ nodes (7th generation) and gyration radius $R_g = 42.6$nm. The values of model parameters were chosen such that they are similar to their values in native proteins: bond length and bead (amino acid) diameter $b = 5 \times 10^{-10}$m, mass of a single bead $m = 4 \times 10^{-25}$Kg, spring natural frequency $\omega_o = 10^{12}$s^{-1}, viscosity of water $\eta = 8.94 \times 10^{-4}$Pa s, and the temperature was set to $T = 298$K. With these parameters the short cutoff, "amino-acid", relaxation time $\tau_0 = \gamma/\omega_o^2 = 3\pi\eta b/(m\omega_o^2) \simeq 10.53$ps is within the range of typical values for proteins [23].

We solve numerically for the exact normal modes and eigen-frequencies of the Sierpinski gasket, and evaluate the pair correlation function according to Eq. (21), in the framework of the Rouse model, for all pairs in the network that are separated by the same distance r within an interval $\delta r = 0.5$A. We then calculate the average value over all such pairs, for each point of time. We have used four values of r: 5,15,25,50 A. The results are shown in Fig. 1.

In Fig. 1(a) we plot, on a log-log scale, the four averaged two-point correlation functions *vs.* the time t. Note the crossover from a constant value, that increases with increasing r as predicted by Eq. (52), to an anomalous subdiffusion time regime, identical to that of the single particle MSD (effectively equal to the correlation function for $r = b = 5$A). In the subdiffusion regime, correlation functions obey Eq. (53) and the behavior is essentially

independent of the distance r. Also note that the crossover time increases with increasing r as implied by Eq. (51). For long times, all curves saturate to the same value. This emerges from the fact that the saturation, $t \to \infty$, limit is always $2 < \vec{u}^2 >_T$, and from the fact that in the Sierpinski gasket averaging over relatively small subset of nodes (i.e. those in the range of $r \pm \delta r$) is approximately identical to any other (say, different r) subset average, or to the complete spatial average.

In order to test the predicted scaling behavior of the two-point correlation function, in particular the version stated in Eq. (56), we normalize the correlation function by $r^{d_w - d_f}$ and the time by $t^*(r)$. The results are shown in Fig. 1(b). Data collapse to a single master curve is observed for times much longer than the shortest ("amino acid") vibrational relaxation time τ_0, and much shorter than the saturation time τ_N. Outside this range, data does not collapse to a single curve. Thus for $r = 5$A, the short time behavior does not obey scaling since for this distance $t^*(r) \simeq \tau_0$. Likewise, all curves diverge from each other close to saturation, $t \sim \tau_N$.

2. Proteins

Next, we perform numerical calculations of the pair correlation function for the protein LysX, PDB code 1UC8, containing $N = 505$ amino acids, using an identical procedure to the one done for the Sierpinski gasket. For this purpose the GNM is used with a cutoff distance $R_c = 6 \times 10^{-10}$m and $m\omega_o^2$ is determined via fit of the mean theoretical (GNM) B-factor value to the experimental value reported in the PDB. Correcting for the over-stiffness of crystalline structures (studied by x-rays) in comparison to structures in solution (studied by NMR), the value of $m\omega_o^2$ is further divided by a factor of four as suggested in Yang *et al.* [40] to yield $m\omega_o^2 = 0.1305$N/m. The mass m is determined separately as the mean amino-acid mass and a value of $m = 1.66 \times 10^{-25}$Kg is obtained. The rest of the parameters are set as in the Sierpinski gasket: bead (amino acid) diameter $b = 5 \times 10^{-10}$m, viscosity of water $\eta = 8.94 \times 10^{-4}$Pa s, and temperature $T = 298$K. Hence the molecular, "amino-acid", time is given by $\tau_0 = \gamma/\omega_o^2 = 32.29$ps. The density of states $g(\omega)$ and mass distribution $M(r)$ of this protein is shown in Ref. [7], from which we have deduced the following values of the fractal and spectral dimension: $d_s = 1.73$, $d_f = 2.51$.

In Fig. 2(a) we plot, on a log-log scale, the averaged two-point correlation functions

vs. the time t, for a few separation distances r. Note again the crossover from a constant value, that increases with increasing r as predicted by Eq. (52), to an effective anomalous subdiffusion time regime, where the crossover time increases with increasing r as implied by Eq. (51). Here, unlike the Sierpinski gasket, curves do not saturate to the same value, showing that the average of $\langle \vec{u}^2 \rangle_T$ over one given subset of amino acids (given r) may not be identical to the average over a different subset (different r), and may also differ from a full spacial average. Moreover, a clear subdiffusion regime is obtained only for the MSD ($r = 0$) due to the fact that τ_N is only a few times larger than $t^*(r)$ (finite size effects) and the low value of the anomalous diffusion exponent ν.

In Fig. 2(b) we normalize the time by r^δ and the correlation function by r^α, and search for the exponents δ and α that collapse the data into a single master curve in the time regime $\tau_0 \ll t \ll \tau_N$. Unlike for the Sierpinski gasket, we avoid using the predicted exponents $\delta = d_w$ (for the Rouse model where $\theta = 2$) and $\alpha = d_w - d_f$, that are supposed to collapse the data. This is because, as found earlier [8], finite size effects lead to modified exponents. Thus our scaling hypothesis is similar to Eq. (56) but with α replacing $d_w - d_f$ and δ replacing d_w (in $t^*(r)$). We find that the values $\alpha = 0.464$ and $\delta = 3.09$ best collapse the data, these values are not too far from the predicted values $\alpha = d_w - d_f = 0.392$ and $\delta = 2.90$ [7]. Thus we can infer the anomalous diffusion exponent for a protein whose topology is identical to LysX but whose size is "infinite", by demanding that for $t \gg t^*(r)$ the dependence on r disappears (ignoring the vanishing algebraically decaying term $\sim r^{2d_f/d_l} t^{-\mu}$). This implies $\Phi_3[u] \sim u^{\alpha/\delta}$ for $u \gg 1$ leading to $\nu = \alpha/\delta = 0.150$, quite close to the predicted exponent $\nu = 1 - d_s/2 = 0.135$.

IV. DYNAMIC STRUCTURE FACTOR

A. Introduction

The dynamic structure factor of complex fluids can be measured by various techniques, e.g, dynamic light scattering [41], inelastic neutron scattering [30], neutron spin-echo [25–27, 42], and x-ray photon correlation spectroscopy [43]. All methods measure dynamic correlations of density fluctuations of the scatterers and each method focuses on a different wavelength range and time regime. Among the four, the two relevant methods for detection

of intramolecular protein dynamics are inelastic neutron scattering and neutron spin-echo. The individual scatterers will be defined here as the individual amino acids, and it will be assumed (as a simple but common approximation) that they all contribute equally to the scattering, irrelevant of their specific identity. The small variation in the scattering properties between one amino acid and the other is supposedly averaged out in the measurement. The structure factor is thus defined in the following way [41]

$$S(\vec{k}, t) = \frac{1}{V} \int_V d^3\vec{r} \int_V d^3\vec{r}\,' e^{i\vec{k}\cdot(\vec{r}-\vec{r}\,')} \langle c(\vec{r}, t) c(\vec{r}\,', 0) \rangle \tag{57}$$

where $c(\vec{r}, t)$ is the stochastic number density, $\vec{k}$ is the scattering wavevector, and V is the macroscopic system volume.

To proceed, one inserts the stochastic number density [41]

$$c(\vec{r}, t) = \sum_i \delta(\vec{r} - \vec{r}_i(t)) , \tag{58}$$

where the sum runs over *all* amino acids in the system, to obtain

$$S(\vec{k}, t) = \frac{1}{V} \sum_{ij} \left\langle e^{i\vec{k}\cdot(\vec{r}_i(t)-\vec{r}_j(0))} \right\rangle . \tag{59}$$

We assume that the system is a dilute solution of N_p individual proteins $\{p\}$, all equivalent, each one having a different, yet random, orientation. Let $\vec{R}_p$ be the center of mass vector of protein p. We therefore have $\vec{r}_i(t) = \vec{R}_p + \vec{R}_{i,p}(t)$ where $\vec{R}_{i,p}$ is the position vector of amino acid i (represented by its α-carbon) in the center of mass coordinate frame of protein p, leading to

$$S(\vec{k}, t) = \frac{1}{V} \sum_{p,p'=1}^{N_p} \left\langle e^{i\vec{k}\cdot\left(\vec{R}_p(t)-\vec{R}_{p'}(0)\right)} \right\rangle \times$$
$$\sum_{ij=1}^{N} \left\langle e^{i\vec{k}\cdot\left(\vec{R}_{i,p}(t)-\vec{R}_{j,p'}(0)\right)} \right\rangle . \tag{60}$$

For dilute solutions, the internal dynamics in each protein is decoupled from the internal dynamics of all other proteins, yet, as they are all identical, it bears exactly the same stochastic evolution. In addition, proteins diffuse independently of each other. Thus, the summation over terms with $p \neq p'$ contributes only to $\vec{k} = 0$ ("forward scattering"), and for $\vec{k} \neq 0$ only terms with $p = p'$ survive to give [41]

$$S(k, t) = \frac{N}{V} \sum_{p=1}^{N_p} \left\langle e^{i\vec{k}\cdot\left(\vec{R}_p(t)-\vec{R}_p(0)\right)} \right\rangle \left\langle S_p(\vec{k}, t) \right\rangle_{\vec{k}} , \tag{61}$$

19

where N is the number of amino acids in a single protein. Here we have defined the single protein structure factor (with $1/N$ normalization factor)

$$S_p(\vec{k}, t) = \frac{1}{N} \left\langle \sum_{i,j=1}^{N} e^{i\vec{k}\cdot\left(\vec{R}_i(t) - \vec{R}_j(0)\right)} \right\rangle , \qquad (62)$$

where $\vec{R}_i$ is the position vector of amino acid i in the center of mass coordinate frame and the sum runs over all amino acids in a single protein. $S_p(k, t) \equiv \left\langle S_p(\vec{k}, t) \right\rangle_{\vec{k}}$ denotes angular averaging, i.e. averaging over all different orientations of the protein with respect to the scattering wavevector $\vec{k}$. This is required since each protein participating as a scattering center is, at any particular time, at random orientation with respect to $\vec{k}$.

If proteins perform simple diffusion in the solvent we find [33, 41]

$$S(k, t) = c\, e^{-k^2 D_{cm} t} S_p(k, t) , \qquad (63)$$

where c is the (mean) amino acid number density, i.e. $c = N c_p$ where $c_p = N_p/V$ is the protein number density, and D_{cm} is the center of mass diffusion coefficient of a single protein. The latter can be estimated using the Stokes-Einstein relation, $D_{cm} \simeq k_B T / 6\pi\eta R_h$, where R_h is the hydrodynamic radius which is approximately proportional to the gyration radius R_g, with a proportionality constant that weakly depends on the number of beads (amino-acids) N and fractal dimension d_f [33, 44, 45]. Rotational diffusion [46] is considered explicitly in the subsequent section and in Appendix B as part of the (ensemble averaged) protein structure factor.

B. Protein structure factor: Exact results

We now calculate the ensemble average structure factor of proteins in dilute solution. First, consider a protein having a fixed but arbitrary orientation with respect to the wavevector $\vec{k}$, with rotational motion arrested. Orientational average will be performed at a later stage. Writing $\vec{R}_i(t) = \vec{R}_{i,\text{eq}} + \vec{u}_i(t)$ we obtain

$$S_p(\vec{k}, t) = \frac{1}{N} \sum_{i,j=1}^{N} e^{i\vec{k}\cdot\left(\vec{R}_{i,\text{eq}} - \vec{R}_{j,\text{eq}}\right)} \left\langle e^{i\vec{k}\cdot(\vec{u}_i(t) - \vec{u}_j(0))} \right\rangle . \qquad (64)$$

Note that, relating to the notations of Secs. II and III, $\vec{u}_i \equiv \vec{u}(\vec{l})$ and $\vec{u}_j \equiv \vec{u}(\vec{l}')$.

Consider now the stochastic variable $\vec{u}_i(t) - \vec{u}_j(0)$. Recall that the dynamics of $\vec{u}_i(t)$ is governed by the linear Langevin equation (11), in which the stochastic force is a white

noise obeying Gaussian statistics. By a general theorem of stochastic processes [47], the statistics of $\vec{u}_i(t)$, being the solution of Eq. (11), is also Gaussian, and so is the combination $\vec{u}_i(t) - \vec{u}_j(0)$. Using the well-known property of Gaussian fluctuations [33, 47], and the isotropy of scalar elasticity (GNM), i.e. the fact that the statistics of all three components of $\vec{u}_i(t)$ is identical, we thus find

$$\left\langle e^{i\vec{k}\cdot(\vec{u}_i(t)-\vec{u}_j(0))} \right\rangle = e^{-\frac{k^2}{6}\langle(\vec{u}_i(t)-\vec{u}_j(0))^2\rangle} . \tag{65}$$

Using Eqs. (65) in Eq. (64) we have, omitting from now on the subscript "eq" in $\vec{R}_{i,\mathrm{eq}}$,

$$S_p(\vec{k},t) = \frac{1}{N} \sum_{i,j=1}^{N} e^{i\vec{k}\cdot(\vec{R}_i-\vec{R}_j)} e^{-\frac{k^2}{6}\langle(\vec{u}_i(t)-\vec{u}_j(0))^2\rangle} . \tag{66}$$

Performing angular averaging we find

$$S_p(k,t) = \frac{1}{N} \sum_{i,j=1}^{N} \frac{\sin[kR_{ij}]}{kR_{ij}} e^{-\frac{k^2}{6}\langle(\vec{u}_i(t)-\vec{u}_j(0))^2\rangle} , \tag{67}$$

where $R_{ij} = |\vec{R}_i - \vec{R}_j|$ is the Euclidean, real-space, distance between amino-acids (represented by their α-carbons) i and j. Eq. (67) is a good starting point for numerical evaluation of both the static ($t = 0$) and dynamic protein structure factor for specific proteins based on their 3D structure. Noteworthy, this expression does not include any unfolding-refolding dynamics which may occur on the sub-microsecond timescale or longer.

When short time rotational diffusion is included, followed by the required angular averaging, the result is (see Appendix B)

$$S_p(k,t) \simeq \frac{1}{N} \sum_{i,j=1}^{N} \langle e^{i\vec{k}\cdot(\vec{R}_i-\vec{R}_j)} e^{-k^2 R_i^2 \sin^2\theta_i D_{\mathrm{rot}} t} \rangle_{\vec{k}} \times$$
$$e^{-\frac{k^2}{6}\langle(\vec{u}_i(t)-\vec{u}_j(0))^2\rangle} , \tag{68}$$

where D_{rot} is the rotational diffusion coefficient ($D_{\mathrm{rot}} t \ll 1$ is assumed), θ_i is the angle between $\vec{k}$ and R_i, and $\langle...\rangle_{\vec{k}}$ means angular average over all directions of $\vec{k}$ at fixed protein orientation. The rotational diffusion coefficient of a protein may be estimated from the Stokes-Einstein-Debye expression [48] $D_{\mathrm{rot}} \simeq k_B T/8\pi\eta R_g^3$. The angular averaging in Eq. (68) requires numerical integration for accurate evaluation. In the following section and Appendix B it is also evaluated approximately to obtain the dominant behavior.

C. Protein structure factor: Approximate results

In this section we present approximate and scaling expressions that can be obtained for fractals and proteins (based on their fractal-like structure). In doing so, we rely on results for the pair correlation function discussed in Sec. III, $\langle (\vec{u}(\vec{\ell}, t) - \vec{u}(\vec{\ell'}, 0))^2 \rangle$ (recall that $\vec{u}_i \equiv \vec{u}(\vec{l})$). The details of the approximations are given in Appendix C.

Consider first the protein static structure factor. To examine the effect of vibrations on the static structure factor we define a "frozen network" structure factor in which vibrations are arrested

$$\tilde{S}_p(k) = \frac{1}{N} \sum_{i,j} \frac{\sin [kR_{ij}]}{kR_{ij}} \,. \tag{69}$$

For $kR_g \gg 1$ we obtain the well known result $\tilde{S}_p(k) \sim k^{-d_f}$, which can be also obtained by scaling approach [19, 33, 49, 50]. When vibrations are included we find, to leading order, the first order correction to $S_p(k) \sim k^{-d_f}$ in the form

$$S_p(k) \approx \tilde{S}_p(k) - \text{const.} \times k^{2-d_w} + \dots \tag{70}$$

However, due to the smallness of the prefactor of the second term, this correction is negligible and $S_p(k) \simeq \tilde{S}_p(k)$.

Next we consider the protein dynamic structure factor. It will be later shown that the rotational diffusion time dependence in $S_p(k, t)$ is rather weak for $t \lesssim \tau_N$. We shall therefore evaluate first the dynamic structure factor with rotational diffusion arrested (Eq. (67)). For short times, $t \ll \tau(k)$, where $\tau(k) \sim k^{-d_f \theta/d_s}$, information did not have time to negotiate a "blob" of linear size $\sim k^{-1}$ and we find that the dynamic structure factor did not decay much and is left almost equal to the static structure factor, $S_p(k, t) \simeq S_p(k)$. A more accurate description yields, to leading order,

$$S_p(k, t) \simeq S_p(k) - \text{const.} \times k^2 \, t^{2/\theta} \,. \tag{71}$$

For the Rouse model ($\theta = 2$) this implies that the short time decay is roughly exponential.

At longer times, $\tau(k) \ll t \ll \tau_N$, i.e. when $1 \ll k\xi(t) \ll kR_g$, information has propagated beyond the scattering wavelength $\sim 1/k$. Physically, this implies that the "blob" of size $\sim 1/k$, that is controlling the relaxation at wavevector $\vec{k}$, is now moving almost coherently as if it was a single bead. This leads to a *stretched exponential* decay of the dynamic structure factor,

$$S_p(k, t) \simeq \tilde{S}_p(k) \exp \left[-(\Gamma_k t)^\nu \right] \tag{72}$$

where

$$\Gamma_k = (B/6)^{1/\nu} k^{2/\nu} \ . \tag{73}$$

Note that the stretching exponent is exactly the anomalous diffusion exponent ν. The stretched exponential decay, together with the dependence of the stretching exponent ν, is thus a strong signature of the fractal structure.

Next we estimate the effect of rotational diffusion using Eq. (68) at short times, $D_{\mathrm{rot}}t \ll 1$. We find that the effect is highly sensitive to the value of k and the observed time regime. Two regimes of time can be distinguished depending on whether $kR_g\sqrt{D_{\mathrm{rot}}t}$ is smaller or larger than unity. If $kR_g\sqrt{D_{\mathrm{rot}}t} \gg 1$, as can occur for very large k's and not too short times, we find in Appendix C that the contribution of rotational diffusion leads, to leading order, to a powerlaw, $\sim t^{-d_f/2}$, pre-exponential factor. Adding translational diffusion according to Eq. (63), we find

$$S(k,t) \approx \text{const. } c \ \tilde{S}_p(k) \ t^{-d_f/2} \exp\left[-(\Gamma_k t)^\nu\right] \times$$
$$\exp\left[-k^2 \frac{k_B T}{6\pi\eta R_g} t\right] \ . \tag{74}$$

In the opposite limit where $kR_g\sqrt{D_{\mathrm{rot}}t} \ll 1$ (but still large wavenumbers $kR_g \gg 1$), we obtain for the combined effect of rotational-translational diffusion

$$S(k,t) \approx c \ \tilde{S}_p(k) \ \exp\left[-(\Gamma_k t)^\nu\right] \times$$
$$\exp\left[-k^2 \frac{3d_f + 4}{12\pi(d_f + 2)} \frac{k_B T}{\eta R_g} t\right] \ . \tag{75}$$

In case that $R_g \gg b$ (not quite the situation for proteins) we have $Bt^\nu \gg (k_B T/\eta R_g)t$ in the relevant time regime $t \ll \tau_N$. In this limit Eq. (75) reduces to a pure stretched exponential decay, $S(k,t) \approx c \ \tilde{S}_p(k) \exp\left[-(\Gamma_k t)^\nu\right]$.

D.   Numerical results for the Sierpinski gasket and proteins

1.   Sierpinski gasket

As done for the pair correlation function, we first evaluate numerically the single particle dynamic structure factor $S_p(k,t)$ for the Sierpinski gasket. Using the single molecule structure factor Eq. (67), where rotational and translational diffusion are arrested, allows us to

focus on the intramolecular vibrations. As argued above, for $kR_g \gg 1$ rotational and translational diffusion have negligible effect in the measurable time regime where the structure factor did not yet decay to a vanishing value. For simplicity and clarity, we use below only the Rouse model of friction, although our conclusions apply equally to the Zimm model. We calculate the dynamic structure factor for four generations of the Sierpinski gasket such that the number of nodes N in the gasket (i.e. gasket "size") varies between $N \simeq 200$ and $N \simeq 7000$.

In Fig. 3 we plot the static and dynamic structure factors for the Sierpinski gasket. The inset shows the static structure factor on a log-log scale for the largest gasket in the series. Note the clear $S_p(k) \sim k^{-d_f}$ powerlaw behavior in the regime $R_g^{-1} \ll k \ll b^{-1}$, showing that vibrations have negligible effect on the static structure factor for realistic spring constants and temperatures. The dynamic structure factor (main figure) of the four gasket generations is shown as $-\log_{10}[S_p(k,t)/\tilde{S}_p(k)]$ *vs.* t/τ_0 on a log-log scale, such that a stretched exponential decay would show on this plot as a straight line whose (positive) slope is the stretching exponent. Note that we divided the dynamic structure factor by the "frozen network" static structure factor, $\tilde{S}_p(k)$, in accord with Eq. (72). The results are presented for a particular wavenumber, $k = 10^{10} \text{m}^{-1}$ for which $kR_g \simeq 426 \gg 1$ for the largest gasket in the series ($N = 6561$), and $kR_g \simeq 53 \gg 1$ for the smallest gasket ($N = 243$). Note that a straight line, whose slope is positive, is formed on an intermediate time window that widen up as we move from a smaller to a larger gasket, demonstrating the diminishing contribution of finite size effects as the system size increases. The stretching exponent that is obtained from the plot, $\beta \simeq 0.325$, is very close to the theoretical value $\beta = \nu = 1 - d_s/2 \simeq 0.317$.

In Fig. 4a we plot the dynamic structure factor for the largest gasket studied ($N = 6561$) for different wavenumbers k, plotting $-\log_{10}[S_p(k,t)/S_p(k,t=0)]$ *vs.* t/τ_0 on a log-log scale. Note that here we divided the dynamic structure factor by the true static structure factor $S_p(k) \equiv S_p(k,t=0)$. This is done in order to verity the quality of the stretched exponential behavior when such an experimental-type analysis of the data is being performed, since $\tilde{S}_p(k)$ is not a measurable quantity, unlike $S_p(k)$. A clear straight line whose slope is positive is formed on an intermediate time window that widens up as k increases. This is in accord with the theoretical prediction associating the stretched exponential behavior with the time regime $\tau(k) \ll t \ll \tau_N$ where $\tau(k) \sim k^{-d_f\theta/d_s} \sim k^{-2.32}$. For the smaller k's studied one can also observe an early exponential-like decay, shown as a straight line with slope $\simeq 1$

on this plot, in accord with Eq. (71). This exponential decay slowly crosses over to the stretched exponential decay. Despite the use of $S_p(k)$ rather than $\tilde{S}_p(k)$, the numerically obtained stretching exponent for the largest k in the series (upper curve), $\beta \simeq 0.30$, is remarkably close the theoretical value $\beta = \nu = 1 - d_s/2 \simeq 0.317$, demonstrating that this experimental-like analysis yields reliable exponents. Fig. 4a is accompanied by Fig. 4b in which we perform local slope analysis. This is done by plotting the first derivative of $\log_{10}[-\log_{10}[S_p(k,t)/S_p(k)]]$ $vs.$ $\log_{10}[t/\tau_0]$. Note the very clear 'shoulders' whose width increase for increasing k, signifying constant slopes in Fig. 4a. Fig. 4b thus provides a complementary assessment of the stretched exponential behavior.

2. Proteins

As done for the Sierpinski gasket, we perform numerical evaluation of the protein dynamic structure factor $S_p(k,t)$, Eq. (67), arresting the rotational and translational diffusion. We study three different proteins of variable sizes: 1FTR ($N = 1184$), 1UC8 ($N = 505$, studied in Sec. III.G.2), and 3TSS ($N = 190$). The GNM is used and parameters are chosen as described in section III.G.2. Parameter values slightly differ form one protein to another and we find: $m\omega_o^2 = 0.1898$, 0.1305, 0.2510N/m and $m = 1.65 \times 10^{-25}$, 1.66×10^{-25}, 1.76×10^{-25}Kg respectively. This leads to the following value of molecular, "amino-acid", time $\tau_0 = \gamma/\omega_o^2 = 22.19$, 32.29, 16.78ps, respectively. The density of states $g(\omega)$ and and mass distribution $M(r)$ of the three proteins is shown in Ref. [7], from which we take the following values of the fractal and spectral dimension: $1FTR - d_s = 1.93$, $d_f = 2.66$; $1UC8 - d_s = 1.73$, $d_f = 2.51$; $3TSS - d_s = 1.52$, $d_f = 2.50$. Since each protein has a different d_s value, we expect a different stretching exponent $\beta = \nu = 1 - d_s/2$ for each one: $\nu = 0.035$, 0.135, 0.24, respectively.

In Fig. 5a we plot the dynamic structure factor of the proteins mentioned above. The theoretical prediction associates a stretched exponential behavior in the time regime $\tau(k) \ll t \ll \tau_N$ that translates to $0.1\tau_0 \ll t \ll 70\tau_0$, and the fitted data shown in Fig. 5a is well within this regime. Indeed, within this intermediate regime the decay is clearly non-exponential, a fingerprint of the fractal-like structure. However, due to finite size effects, the stretching exponents (i.e. the slopes) obtained from the fits, $\beta = 0.119, 0.1584, 0.199$ respectively, deviate from the predicted values of ν stated above. Fig. 5a is accompanied

by Fig. 5b in which we perform local slope analysis. This is done by plotting the first derivative of $\log_{10}[-\log_{10}[S_p(k,t)/S_p(k)]]$ *vs.* $\log_{10}[t/\tau_0]$. It is possible to observe very weak shoulders, signifying the existence of roughly constant slopes, in the regimes that correspond to the fitted regimes in Fig. 5a (apparently more visible for 3TSS). It appears that finite size effects are strong in proteins and that a pure stretched exponential behavior is hardly obtained when we consider vibrations alone. Although one could have naively expected (in analogy with the Sierpinski gasket) that for proteins with ~ 1000 amino acids or more (e.g., 1FTR in this study) finite size effects would be less significant, this is not the case. As it turns out, in such proteins the value of d_s is usually very close to 2, consequently leading to vanishing stretching exponents ν. Such an exponent is difficult to determine accurately as it is highly sensitive to the short and long time, non-stretched-exponential, dynamics. Nevertheless, the values obtained from our fits of the effective exponents quantify the non-exponential behavior as a whole. Since the GNM (and hence our numerical calculations) are solely based on protein structure, the non-exponential behavior we observe is a direct manifestation of the fractal-like structure of proteins.

3. Proteins: Including rotational and translational diffusion and comparison with neutron spin-echo experiments

Next we further examine the decay of the dynamic structure factor when rotational and translational diffusion are included. Consider first the effect of rotational diffusion for the above three proteins. Adding rotational diffusion according to Eq. (68) (or Eq. (B11)), using $R_h = R_g$ where R_g is calculated from the PDB structure, we plot in Fig. 6 $-\log_{10}[S_p(k,t)/S_p(k)]$ *vs.* t/τ_0 on a log-log scale. We observe a clear, effective, stretched exponential decay of the dynamic structure factor in an intermediate time regime, yielding stretching exponents $\beta = 0.34, 0.28, 0.32$ for 3TSS, 1UC8, and 1FTR respectively. Note that these exponents are higher than those obtained from vibrations alone. The inset in Fig. 6 includes also the contribution of translational diffusion using again $R_h = R_g$. Following Ref. [27], we define $t_0 = 0.01ns$, and plot $S(k,t)/S(k,t_0)$ *vs.* the time in nano-seconds. The cumulative effect of all three dynamical processes gives rise to a non-exponential decay that can be well fitted by a stretched exponential in the time interval $t \in [0.01ns, 1ns]$. The effective stretching exponents are $\beta = 0.72, 0.42, 0.65$ for 3TSS, 1UC8 and 1FTR respectively,

and are significantly higher than those obtained from vibrations and rotations alone. We conclude that, in proteins, the exact value of the effective stretching exponent is sensitive to the interplay between vibrations, rotations and translations.

Next we consider two proteins, horse heart myoglobin (Mb, PDB code 3LR7) and bovine hemoglobin (Hb, PDB code 2QSP), that have been recently investigated in dilute solutions by neutron spin-echo. Analyzing the vibrational density of states of these proteins we find $d_s = 1.56$ for Mb and $d_s = 1.74$ for Hb, leading to $\nu = 1 - d_s/2 = 0.22$, 0.13 for Mb and Hb, respectively. Adding translational and rotational diffusion, and normalizing the dynamic structure factor by the effective static structure factor at $t =$ 10ps (similar to the procedure in Ref. [27]), we find that for the experimental value of k, $k = 0.579\text{A}^{-1}$, an effective stretched exponential decay is obtained in the experimental time window $10\text{ps} \leq t \leq 1\text{ns}$, with stretching exponents $\beta = 0.89$ (Mb) $\beta = 0.86$ (Hb). These exponents are quite close to unity, suggesting that in the case of these two proteins, either that effect the vibrations have been underestimated or that the translational-rotational effect has been overestimated. Support for the latter possibility appears in the data of Ref. [27] that shows that the translational diffusion coefficient is concentration dependent, suggesting that the solution is (perhaps) not sufficiently dilute to prevent aggregation (oligomerization) of proteins so that aggregate (oligomer) diffusion coefficients should be used instead of those of individual proteins. Another possibility that can lead to a large hydrodynamic radius is the formation of a thick hydration shell. Exploring this option we introduce an effective radius R_g^*, vary it between the single protein value R_g and 4 times this value, and use it to evaluate D_{rot} and D_{cm}. We find that for $R_g^* \simeq 4R_g$, the stretching exponent lowers to $\beta \simeq 0.75$. Moreover, increasing slightly the value of k to $k = 1\text{A}^{-1}$ the stretching exponent further goes down to $\beta \simeq 0.52$. This shows that the exact value of the stretching exponent is not universal and results from an interplay between vibrations, rotations, and translations. However, it is gratifying that one can obtain a low value of β, due to the very low value of ν that serves as an effective lower bound for β.

V. CONCLUSIONS

We have integrated and advanced upon our previous studies on the vibrational dynamics of fractals in general, and of proteins as fractals, and presented a through study of the

dynamic structure factor $S(k, t)$ of vibrating fractals and proteins in dilute solutions. Our study is highly detailed and may allow comprehensive comparison with experiment. Our main result is however simple and shows that so long as $kR_g \gg 1$ and $k\bar{u} \gtrsim 1$, where $\bar{u} \equiv \sqrt{\langle u^2 \rangle}$, and with rotational and translational degrees of freedom arrested, the decay of the dynamic structure factor is strongly influenced by the anomalous diffusion of amino acids (beads) at short times, $\langle \Delta \vec{u}(t)^2 \rangle = B\, t^\nu$. The value of ν depends on the fractal (d_f) and spectral (d_s) dimensions, $\nu = 1 - d_s/2$ in the Rouse model of friction and $\nu = (2 - d_s)/(2 - d_s + d_s/d_f)$ in the Zimm model, and those are easily calculated for proteins based on their published PDB structures [7, 51]. This anomalous diffusion is thus a direct signature of the fractal structure of proteins. The result for large proteins (fractals) is a stretched exponential decay of the dynamic structure factor, $S(k, t) \approx S(k) \exp\left[-(\Gamma_k t)^\beta \right]$, with anomalous k dependence of the relaxation rate, $\Gamma_k \sim k^{2/\beta}$, and a stretching exponent β that identifies with the anomalous diffusion exponent ν. Besides proteins, our theory can be used for other systems exhibiting fractal structures, e.g., colloidal gels [52], chromatin [53], and colloidal glasses [54].

The anomalous wavenumber dependence of the relaxation rate, $\Gamma_k \sim k^{2/\nu}$, and the anomalous diffusion, $\langle \Delta \vec{u}(t)^2 \rangle \sim t^\nu$, can be explained using simple scaling hypotheses. For the relaxation rate we assume $\Gamma_k = Dk^2 h(k\bar{u})$, where $h(x)$ is a scaling function and D is the center of mass diffusion coefficient of the fractal. Note that the scaling variable is $k\bar{u}$ rather than kR_g, as for flexible polymers. We make use of the generalized Landau-Peierls instability, $\bar{u} \sim N^{1/d_s - 1/2}$, and take $D \sim N^{-1}$ and $D \sim R_g^{-1} \sim N^{-1/d_f}$ for the Rouse and Zimm type models of friction [33], respectively. Demanding that Γ_k is independent of N for $k\bar{u} \gg 1$, the scaling function for $x \gg 1$ must satisfy $h(x) \sim x^{2d_s/(2-d_s)}$ (for the Rouse model) and $h(x) \sim x^{2d_s/[d_f(2-d_s)]}$ (for the Zimm model), leading to $\Gamma_k \sim k^{2/\nu}$ with $\nu = 1 - d_s/2$ (Rouse) and $\nu = (2 - d_s)/(2 - d_s + d_s/d_f)$ (Zimm) as stated. Similarly, for the MSD we assume $\langle \Delta \vec{u}(t)^2 \rangle = \bar{u}^2 \phi(t/\tau_N)$ where $\phi(x)$ is the scaling function and τ_N is the longest vibrational relaxation time. Assuming $\tau_N \simeq \bar{u}^2/D$, such that $\tau_N \sim N^{2/d_s}$ (Rouse) and $\tau_N \sim N^{2/d_s - 1 + 1/d_f}$ (Zimm), and demanding that for $t \ll \tau_N$ the MSD is independent of N, it follows that $\phi(x) \sim x^\nu$ for $x \ll 1$ (with ν taking the above stated values associated with the Rouse and Zimm models) leading to $\langle \Delta \vec{u}(t)^2 \rangle \sim t^\nu$.

Numerical evaluation for proteins in solutions demonstrates that the small size of most proteins, combined with the influence of rotational and translational diffusion processes,

leads to significant deviations of the value of β from its "infinite network" limit ν. Nevertheless, β remains a fingerprint of the fractal nature of proteins. Moreover, ν influences the value of β, and serves as an effective lower bound for it. Comparison with recent neutron spin-echo studies on hemoglobin and myoglobin is not entirely satisfactory and may motivate further studies in this direction. As a practical conclusion we suggest to perform such experiments with proteins bounded to a surface [55, 56] in similarity to what was done in [57]. This will diminish to a minimum the contribution from translational and rotational degrees of freedom and will thus allow for better exploration of internal degrees of freedom.

VI. ACKNOWLEDGMENTS

Appendix A: Proof of Eq. (39)

1. Disorder averaged correlation functions

To prove Eq. (39) we develop the correlation functions in this equation. Note that here it is implicitly assumed that disorder average/spatial average (summing over $\vec{\ell}$ and $\vec{\ell'}$ and dividing by N^2) is being performed in addition to the thermal/time average. This eliminates any real positional dependence, leaving only the relative distance between the two amino acids as a variable. It is easy to show that

$$\langle (\vec{u}(\vec{\ell},t) - \vec{u}(\vec{\ell'},0))^2 \rangle = \langle \vec{u}(\vec{\ell},t)^2 \rangle + \langle \vec{u}(\vec{\ell'},0)^2 \rangle$$
$$-2\langle \vec{u}(\vec{\ell},t) \cdot \vec{u}(\vec{\ell'},0) \rangle =$$
$$2\langle \vec{u}^{\,2} \rangle - 2\langle \vec{u}(|\vec{\ell} - \vec{\ell'}|,t) \cdot \vec{u}(0,0) \rangle \qquad (A1)$$

$$\langle \Delta\vec{u}(t)^2 \rangle = 2\langle \vec{u}^{\,2} \rangle - 2\langle \vec{u}(0,t) \cdot \vec{u}(0,0) \rangle \qquad (A2)$$

$$\langle \vec{x}(t) \cdot \vec{x}(0) \rangle = \langle (\vec{u}(\vec{\ell},t) - \vec{u}(\vec{\ell'},t)) \cdot (\vec{u}(\vec{\ell},0) - \vec{u}(\vec{\ell'},0)) \rangle =$$

$$\langle \vec{u}(\vec{\ell},t) \cdot \vec{u}(\vec{\ell},0) \rangle + \langle \vec{u}(\vec{\ell'},t) \cdot \vec{u}(\vec{\ell'},0) \rangle -$$

$$\langle \vec{u}(\vec{\ell},t) \cdot \vec{u}(\vec{\ell'},0) \rangle - \langle \vec{u}(\vec{\ell'},t) \cdot \vec{u}(\vec{\ell},0) \rangle =$$

$$2\langle \vec{u}(0,t) \cdot \vec{u}(0,0) \rangle - 2\langle \vec{u}(|\vec{\ell} - \vec{\ell'}|,t) \cdot \vec{u}(0,0) \rangle .$$

$$(A3)$$

Using the above three equations in Eq. (39) leads to an identity.

2. Exact correlation functions

Here we derive an expression that is equivalent to Eq. (39) using exact correlation functions. To do so, first consider the combination of two-point correlation functions $\langle (\vec{u}(\vec{\ell},t) - \vec{u}(\vec{\ell'},0))^2 \rangle + \langle (\vec{u}(\vec{\ell'},t) - \vec{u}(\vec{\ell},0))^2 \rangle$, that is symmetric for exchange between $\vec{\ell}$ and $\vec{\ell'}$ (regardless of the present, model-dependent, symmetry of each one),

$$\langle (\vec{u}(\vec{\ell},t) - \vec{u}(\vec{\ell'},0))^2 \rangle + \langle (\vec{u}(\vec{\ell'},t) - \vec{u}(\vec{\ell},0))^2 \rangle =$$

$$\langle \vec{u}(\vec{\ell},t)^2 \rangle + \langle \vec{u}(\vec{\ell'},t)^2 \rangle + \langle \vec{u}(\vec{\ell},0)^2 \rangle + \langle \vec{u}(\vec{\ell'},0)^2 \rangle$$

$$-2\langle \vec{u}(\vec{\ell},t) \cdot \vec{u}(\vec{\ell'},0) \rangle - 2\langle \vec{u}(\vec{\ell'},t) \cdot \vec{u}(\vec{\ell},0) \rangle =$$

$$2\langle \vec{u}(\vec{\ell})^2 \rangle + 2\langle \vec{u}(\vec{\ell'})^2 \rangle$$

$$-2\langle \vec{u}(\vec{\ell},t) \cdot \vec{u}(\vec{\ell'},0) \rangle - 2\langle \vec{u}(\vec{\ell'},t) \cdot \vec{u}(\vec{\ell},0) \rangle . \qquad (A4)$$

Next, consider the MSDs of the specific (non-disorder averaged) amino acids $\vec{\ell}$ and $\vec{\ell'}$,

$$\langle \Delta \vec{u}(\vec{\ell},t)^2 \rangle = 2\langle \vec{u}(\vec{\ell})^2 \rangle - 2\langle \vec{u}(\vec{\ell},t) \cdot \vec{u}(\vec{\ell},0) \rangle , \qquad (A5)$$

$$\langle \Delta \vec{u}(\vec{\ell'},t)^2 \rangle = 2\langle \vec{u}(\vec{\ell'})^2 \rangle - 2\langle \vec{u}(\vec{\ell'},t) \cdot \vec{u}(\vec{\ell'},0) \rangle . \qquad (A6)$$

Finally, consider the autocorrelation function of the fluctuations in distance $\langle \vec{x}(\vec{\ell},\vec{\ell'},t)$ between the specific amino acids $\vec{\ell}$ and $\vec{\ell'}$,

$$\langle \vec{x}(\vec{\ell},\vec{\ell'},t) \cdot \vec{x}(\vec{\ell},\vec{\ell'},0) \rangle =$$

$$\langle (\vec{u}(\vec{\ell},t) - \vec{u}(\vec{\ell'},t)) \cdot (\vec{u}(\vec{\ell},0) - \vec{u}(\vec{\ell'},0)) \rangle =$$

$$\langle \vec{u}(\vec{\ell},t) \cdot \vec{u}(\vec{\ell},0) \rangle + \langle \vec{u}(\vec{\ell'},t) \cdot \vec{u}(\vec{\ell'},0) \rangle -$$

$$\langle \vec{u}(\vec{\ell},t) \cdot \vec{u}(\vec{\ell'},0) \rangle - \langle \vec{u}(\vec{\ell'},t) \cdot \vec{u}(\vec{\ell},0) \rangle .$$

$$(A7)$$

Combining Eqs. (A4)-(A7), and using now the symmetry for exchange between $\vec{\ell}$ and $\vec{\ell'}$, $\langle(\vec{u}(\vec{\ell},t) - \vec{u}(\vec{\ell'},0))^2\rangle = \langle(\vec{u}(\vec{\ell'},t) - \vec{u}(\vec{\ell},0))^2\rangle$, that follows from Eq. (21), leads to the following identity

$$\langle(\vec{u}(\vec{\ell},t) - \vec{u}(\vec{\ell'},0))^2\rangle =$$
$$\frac{1}{2}\left[\langle\Delta\vec{u}(\vec{\ell},t)^2\rangle + \langle\Delta\vec{u}(\vec{\ell'},t)^2\rangle\right] + \langle\vec{x}(\vec{\ell},\vec{\ell'},t) \cdot \vec{x}(\vec{\ell},\vec{\ell'},0)\rangle .$$

(A8)

Appendix B: Effect of rotational diffusion

Here we evaluate approximately the effect of protein rotations on the dynamic structure factor for short times. An alternative, more complete, calculation, can be found in Ref. [46], however, the approximate calculation below suffices for our purposes. Rotations result in a change of the angle between the wavevector $\vec{k}$ and the vector of each residue i, $\vec{R}_i(t)$, in the protein center of mass coordinate frame. At $t = 0$ this angle is a random variable, changing from one protein to the other within the scattering ensemble. As a result of protein rotational diffusion, this angle is changing with time and we may describe this change by the unit vector $\hat{n}_i(t)$ which denotes the direction of the vector $\vec{R}_i(t)$, $\vec{R}_i(t) = R_i\hat{n}_i(t)$, where it is understood that the dependence on time in $\vec{R}_i(t)$ is *solely due to rotations*, as vibrations are included separately. Consider the average

$$\langle...\rangle \equiv \langle e^{i\vec{k}\cdot\left(\vec{R}_i(t) - \vec{R}_j(0)\right)}\rangle .$$

(B1)

Accordingly we write $\vec{R}_i(t) = \vec{R}_i(0) + R_i\left(\hat{n}_i(t) - \hat{n}_i(0)\right)$ leading to

$$\langle...\rangle = e^{i\vec{k}\cdot\left(\vec{R}_i - \vec{R}_j\right)}\langle e^{iR_i\vec{k}\cdot(\hat{n}_i(t) - \hat{n}_i(0))}\rangle$$

(B2)

where, for brevity, we have defined $\vec{R}_i = \vec{R}_i(0)$ and $\vec{R}_j = \vec{R}_j(0)$.

At early times, $D_{\rm rot}t \ll 1$, where $D_{\rm rot}$ is the rotational diffusion coefficient, the vector $\vec{s}_i(t) = \hat{n}_i(t) - \hat{n}_i(0)$ is almost perpendicular to $\hat{n}_i(0)$, being almost tangent to the unit sphere at $\hat{n}_i(0)$. Its radial component, along $\hat{n}_i(0)$ is negligible. Hence this 2D vector represent a 2D (almost) regular diffusion, and its two components are independent and obey almost exactly Gaussian statistics. We denote by $\vec{k}_t$ the 2D projection of $\vec{k}$ on the plane that is tangent to the unit sphere at $\hat{n}_i(0)$, so that the magnitude of $\vec{k}_t$ is $k_t = k\sin\theta_i$ where θ_i is

the angle between $\vec{k}$ and R_i. Using these definitions

$$\langle ...\rangle \simeq e^{i\vec{k}\cdot\left(\vec{R}_i-\vec{R}_j\right)}\langle e^{iR_i\vec{k}_t\cdot\vec{s}_i(t)}\rangle \ . \tag{B3}$$

Thus, using the nearly Gaussian statistics property of the 2D vector $\vec{s}_i(t)$,

$$\langle ...\rangle \simeq e^{i\vec{k}\cdot\left(\vec{R}_i-\vec{R}_j\right)}e^{-\frac{1}{4}k_t^2 R_i^2\langle \vec{s}_i(t)^2\rangle} \ . \tag{B4}$$

Here we require the calculation of the unit vector MSD

$$\langle \vec{s}_i(t)^2\rangle = \langle (\hat{n}_i(t)-\hat{n}_i(0))^2\rangle = 2\left(1-\langle \hat{n}_i(t)\cdot\hat{n}_i(0)\rangle\right) \ . \tag{B5}$$

In rotational diffusion theory one finds [33]

$$\langle \hat{n}_i(t)\cdot\hat{n}_i(0)\rangle = e^{-2D_{\rm rot}t} \ , \tag{B6}$$

where $D_{\rm rot}$ is the rotational diffusion coefficient. Hence

$$\langle (\hat{n}_i(t)-\hat{n}_i(0))^2\rangle = 2\left(1-e^{-2D_{\rm rot}t}\right) \simeq 4D_{\rm rot}t \ , \tag{B7}$$

where the last equality holds for short times $D_{\rm rot}t \ll 1$. This shows that rotation angle $\delta\Omega(t)$ between $\hat{n}_i(t)$ and $\hat{n}_i(0)$ obeys $\langle \delta\Omega(t)^2\rangle \simeq 4D_{\rm rot}t$.

Using these results in the dynamic structure factor that now includes both rotations (as $\vec{R}_i(t)$) and vibrations

$$S_p(\vec{k},t) \simeq \frac{1}{N}\sum_{i,j}\left\langle e^{i\vec{k}\cdot\left(\vec{R}_i(t)-\vec{R}_j(0)\right)}\right\rangle e^{-\frac{k^2}{6}\langle (\vec{u}_i(t)-\vec{u}_j(0))^2\rangle} \ , \tag{B8}$$

leads to

$$S_p(\vec{k},t) \simeq \frac{1}{N}\sum_{i,j}I(\vec{k},t)e^{-\frac{k^2}{6}\langle (\vec{u}_i(t)-\vec{u}_j(0))^2\rangle} \ . \tag{B9}$$

where

$$I(\vec{k},t) = e^{ikR_{ij}\cos\theta_{ij}}\exp\left[-k^2R_i^2\sin^2\theta_i D_{\rm rot}t\right] \ , \tag{B10}$$

and θ_{ij} is the angle between $\vec{k}$ and $\vec{R}_{ij}\equiv\vec{R}_i-\vec{R}_j$. Performing the angular average over the initial angles is equivalent to rotating the wavevector $\vec{k}$ in all directions, yielding $\langle I(\vec{k},t)\rangle_{\vec{k}}$ and thus $\langle S_p(\vec{k},t)\rangle_{\vec{k}}$. Since one has to keep the angle between the vectors R_i and R_j fixed, this implies that the angles θ_i and θ_{ij} are dependent. Therefore, for accurate analysis we turn to numerical evaluation. The angularly averaged dynamics structure factor (excluding translational diffusion) is thus

$$S_p(k,t) = \frac{1}{N}\sum_{i,j}\langle I(\vec{k},t)\rangle_{\vec{k}}e^{-\frac{k^2}{6}\langle (\vec{u}_i(t)-\vec{u}_j(0))^2\rangle} \ . \tag{B11}$$

Eq. (B11) allows to estimate the effect of rotational diffusion at short times, $D_{\rm rot}t \ll 1$.

Appendix C: Protein structure factor – derivation of approximate results

Here we evaluate approximately Eq. (68) using the two-point correlation function derived in Sec. III. As Eqs. (52)-(53) already involve positional averaging, we may ignore details of the protein structure.

1. Static structure factor

Consider first the static structure factor

$$S_p(k) = \frac{1}{N} \sum_{i,j=1}^{N} \frac{\sin[kR_{ij}]}{kR_{ij}} \exp\left[-\frac{k^2}{6} C \frac{k_B T}{m\omega_o^2} \left(\frac{R_{ij}}{b}\right)^{d_w - d_f}\right] . \tag{C1}$$

To examine the effect of vibrations on the static structure factor we also define a "frozen network" structure factor that does not include the vibrational contributions

$$\tilde{S}_p(k) = \frac{1}{N} \sum_{i,j} \frac{\sin[kR_{ij}]}{kR_{ij}} . \tag{C2}$$

If the network is assumed "infinitely" large we can ignore (as in Eqs. (52)-(53)) boundary effects, and perform the summation over j. Transforming the sum to an integral we may formally write

$$S_p(k) = \frac{1}{b^{d_f}} \int_{V_g} d^{d_f} r \frac{\sin[kr]}{kr} \exp\left[-\frac{k^2}{6} C \frac{k_B T}{m\omega_o^2} \left(\frac{r}{b}\right)^{d_w - d_f}\right] . \tag{C3}$$

and similarly for $\tilde{S}_p(k)$ (with the second, exponential, term in the integrand equal to unity). For $kR_g \gg 1$ and in case of a "frozen network" this leads to the well known result $\tilde{S}_p(k) \sim k^{-d_f}$, as can be also obtained by scaling approach. More precisely,

$$\tilde{S}_p(k) \simeq \frac{\pi^{(d_f+1)/2} 2^{d_f-1}}{\Gamma\left[\frac{3}{2} - \frac{d_f}{2}\right] b^{d_f}} k^{-d_f} . \tag{C4}$$

Yet, some contribution, even if small, is obtained from the vibrations, similar to the broadening of the x-ray Brag peaks. Expanding the second term in the integrand of Eq. (C3) to leading order we obtain the first order correction to $S_p(k) \sim k^{-d_f}$ in the form

$$\begin{aligned}
S_p(k) \approx{}& \tilde{S}_p(k) \\
&- \frac{C d_f \pi^{(d_f+1)/2} 2^{d_w-1} \Gamma[1+d_w/2]}{6 d_w \Gamma[1+d_f/2] \Gamma\left[\frac{3}{2} - \frac{d_w}{2}\right]} \frac{k_B T}{m\omega_o^2 b^{d_w}} k^{2-d_w} \\
&+ \quad \dots \quad .
\end{aligned} \tag{C5}$$

2. Dynamic structure factor: Vibrations

Next we consider the dynamic structure factor. It will be later shown that the rotational diffusion time dependence in $S_p(q,t)$ is rather weak for $t \lesssim \tau_N$. Taking this as an assumption for now, the dominant relaxation is due to vibrations. For the first level of analysis, we shall therefore ignore rotational diffusion and use Eq. (67).

For short times, $t \ll \tau(k)$, where $\tau(k) = t^*(r = k^{-1}) \simeq \bar{A}^{-1}\omega_o^{-\theta}(kb)^{-d_f\theta/d_s}$, we may use Eq. (52) to find that the dynamic structure factor did not decay much and is left almost equal to the static structure factor, $S_p(k,t) \simeq S_p(k)$. A more accurate description may be obtained as follows. For all pairs for which "information" has already propagated between them, $R_{ij} < \xi(t) < 1/k$, we should use Eq. (53). For all pairs for which information has not yet arrived, $\xi(t) < R_{ij}$, we should use Eq. (52). Thus

$$
S_p(k,t) = \frac{1}{N} \sum_{i,j;R_{ij}<\xi(t)}^{N} \frac{\sin[kR_{ij}]}{kR_{ij}} \exp\left[-\frac{k^2}{6}B\,t^\nu\right] \times
$$
$$
\exp\left[-\frac{k^2}{6}C_1\frac{k_BT}{m\omega_o^{d_s}}\,(R_{ij}/b)^{2d_f/d_l}\,(\bar{A}t)^{-\mu}\right]
$$
$$
+\frac{1}{N} \sum_{i,j;R_{ij}>\xi(t)}^{N} \frac{\sin[kR_{ij}]}{kR_{ij}} \exp\left[-\frac{k^2}{6}C\frac{k_BT}{m\omega_o^2}\left(\frac{R_{ij}}{b}\right)^{d_w-d_f}\right].
$$
(C6)

It appears as a very good approximation to set the third, exponential, term in the sum running on $R_{ij} < \xi(t)$ to unity, since its argument is much smaller than one in the relevant timescales. Transforming the sum running on pairs with $R_{ij} < \xi(t)$ to an integral and evaluating the integral approximately for $k\xi(t) \ll 1$, Eq. (67) becomes

$$
S_p(k,t) \simeq \frac{\pi^{d_f/2}}{\Gamma[d_f/2+1]b^{d_f}}\xi(t)^{d_f} \times
$$
$$
\left(1 - \frac{d_f}{6(2+d_f)}k^2\xi(t)^2 + ...\right)\exp\left[-\frac{k^2}{6}B\,t^\nu\right] +
$$
$$
\frac{1}{N}\sum_{i,j;R_{ij}>\xi(t)}^{N}\frac{\sin[kR_{ij}]}{kR_{ij}}\exp\left[-\frac{k^2}{6}C\frac{k_BT}{m\omega_o^2}\left(\frac{R_{ij}}{b}\right)^{d_w-d_f}\right].
$$
(C7)

Equivalently,

$$
S_p(k,t) \simeq S_p(k) - \frac{\pi^{d_f/2}}{\Gamma[d_f/2+1]b^{d_f}}\xi(t)^{d_f} \times
$$

$$\left(1 - \frac{d_f}{6(2+d_f)}k^2\xi(t)^2 + ...\right)\left(1 - \exp\left[-\frac{k^2}{6}B\ t^\nu\right]\right) \ ,$$

(C8)

which, using $\xi(t) \simeq \ell(t)^{d_l/d_f} \simeq \omega_o^{d_s/d_f}(\bar{A}t)^{\frac{d_s}{d_f\theta}}$ and expanding for short times (using $\nu + d_s/\theta = 2/\theta$), yields, to leading order,

$$S_p(k,t) \simeq S_p(k) - C_3\ k^2\ t^{2/\theta} \ ,$$

(C9)

where

$$C_3 = \frac{\pi^{d_f/2}}{6\Gamma[d_f/2+1]b^{d_f}}\omega_o^{d_s}\bar{A}^{\frac{d_s}{\theta}}B \ .$$

(C10)

Note that for the Rouse model ($\theta = 2$) this implies that the short time decay is roughly exponential.

At longer times, $\tau(k) \ll t \ll \tau_N$, i.e. when $1 \ll k\xi(t) \ll kR_g$ such that information has propagated beyond the scattering wavelength $\sim 1/k$, we may use Eq. (53) in Eq. (67). This is true even though the sum in Eq. (67) include all pairs, thus it includes also pairs for which information has not yet propagated between them and hence obeying Eq. (52). However, these pairs are distant much further than $1/k$ apart, $k^{-1} \ll \xi(t) \ll R_{ij}$, hence they contribute a vanishingly small value to the sum due to the familiar property of the Fourier transform. Physically, this implies that the "blob" of size $\sim 1/k$, which is controlling the relaxation at wavevector $\vec{k}$, is moving almost together as if it was a single bead. This leads (setting again the third, exponential, term in the sum running on $R_{ij} < \xi(t)$ to unity) to a *stretched exponential* decay of the dynamic structure factor,

$$S_p(k,t) \simeq \tilde{S}_p(k)\ \exp\left[-\frac{k^2}{6}B\ t^\nu\right] \ ,$$

(C11)

where $\tilde{S}_p(k)$ is the "frozen fractal" static structure factor. As shown above, for not too soft vibrations $\tilde{S}_p(k) \simeq S_p(k)$. Equivalently, this result may be written as

$$S_p(k,t) \simeq \tilde{S}_p(k)\ \exp\left[-\frac{k^2}{6}\langle\Delta\vec{u}(t)^2\rangle\right] \ ,$$

(C12)

or, more conveniently, as

$$S_p(k,t) \simeq \tilde{S}_p(k)\ \exp\left[-(\Gamma_k t)^\nu\right] \ ,$$

(C13)

where

$$\Gamma_k = (B/6)^{1/\nu}k^{2/\nu} \ .$$

(C14)

The stretched exponential decay, together with the dependence of the stretching exponent ν, is thus a strong signature of the fractal structure.

3. Dynamic structure factor: Vibrations and rotational diffusion

To estimate the corrections to this result due to rotational diffusion, c.f. Eq. (68), we first introduce a decoupling approximation to the angular average of $\langle I(\vec{k},t)\rangle$, Eq. (B10),

$$\langle I(\vec{k},t)\rangle_{\vec{k}} \simeq \langle e^{ikR_{ij}\cos\theta_{ij}}\rangle_{\vec{k}}\langle \exp\left[-k^2R_i^2\sin^2\theta_i D_{\mathrm{rot}}t\right]\rangle_{\vec{k}} , \tag{C15}$$

in which we ignore the coupling between the angles θ_{ij} and θ_i. Thus we can use

$$\langle e^{ikR_{ij}\cos\theta_{ij}}\rangle_{\vec{k}} = \frac{\sin\left[kR_{ij}\right]}{kR_{ij}} \tag{C16}$$

and

$$\langle \exp\left[-k^2R_i^2\sin^2\theta_i D_{\mathrm{rot}}t\right]\rangle_{\vec{k}} = \frac{F[kR_i\sqrt{D_{\mathrm{rot}}t}]}{kR_i\sqrt{D_{\mathrm{rot}}t}} , \tag{C17}$$

where $F[x]$ is the Dawson integral defined by $F(x) = e^{-x^2}\int_0^x dy\, e^{y^2}$. Next we take the "infinite" fractal limit, and replace sums by integrals, to obtain

$$S_p(k,t) \simeq \frac{1}{N}\exp\left[-\frac{k^2}{6}B\ t^\nu\right]\frac{1}{b^{2d_f}}\int_{V_g} d^{d_f}r\int_{V_g}d^{d_f}r' \times$$
$$\frac{\sin\left[k|\vec{r}-\vec{r}\,'|\right]}{k|\vec{r}-\vec{r}\,'|}\frac{F\left[kr'\sqrt{D_{\mathrm{rot}}t}\right]}{kr'\sqrt{D_{\mathrm{rot}}t}} \times$$
$$\exp\left[-\frac{k^2}{6}C_1\frac{k_BT}{m\omega_o^{d_s}}\ (|\vec{r}-\vec{r}\,'|/b)^{2d_f/d_l}\ (\bar{A}t)^{-\mu}\right] . \tag{C18}$$

We now assume *very large* k such that $kR_g\sqrt{D_{\mathrm{rot}}t} \gg 1$ (although our short time assumption $D_{\mathrm{rot}}t \ll 1$ still holds). Integrating over r' leads to

$$S_p(k,t) \simeq \frac{d_f\pi^{3/2+d_f/2}\mathrm{Csc}[d_f\pi/2]}{4Nb^{2d_f}\Gamma[3/2-d_f/2]\Gamma[d_f/2+1]D_{\mathrm{rot}}^{d_f/2}} \times$$
$$k^{-d_f}\ t^{-d_f/2}\exp\left[-\frac{k^2}{6}B\ t^\nu\right] \times$$
$$\int_{V_g}d^{d_f}r\frac{\sin\left[kr\right]}{kr}\exp\left[-\frac{k^2}{6}C_1\frac{k_BT}{m\omega_o^{d_s}}\ (r/b)^{2d_f/d_l}\ (\bar{A}t)^{-\mu}\right] . \tag{C19}$$

Integrating over r, and expanding the second, exponential, term in the integrand to leading order, we find

$$S_p(k,t) \approx \mathrm{const}.k^{-d_f}\ t^{-d_f/2}\ \exp\left[-\frac{k^2}{6}B\ t^\nu\right] \times$$
$$\left(\tilde{S}_p(k) - \mathrm{const}.\frac{k_BT}{m\omega_o^{d_s}b^{2d_f/d_l}}k^{2-d_f-2d_f/d_l}(\bar{A}t)^{-\mu}\right) . \tag{C20}$$

36

Thus we find that, to leading order, the dynamics structure factor decays according to

$$S_p(k,t) \approx t^{-d_f/2} \exp\left(-\frac{1}{6}k^2 B t^\nu\right) \approx t^{-d_f/2} \exp\left[-(\Gamma_k t)^\nu\right] . \qquad \text{(C21)}$$

In the case of not so large k or very short times, such that $kR_g\sqrt{D_{\text{rot}}t} \ll 1$ (but still $kR_g \gg 1$), we find, to leading order,

$$S_p(k,t) \approx \exp\left[-\frac{k^2}{6}B\ t^\nu\right]\left(1 - \frac{2d_f}{3(2+d_f)}k^2 R_g^2 D_{\text{rot}}t\right) \times$$
$$\left(\tilde{S}_p(k) - \text{const.}\frac{k_B T}{m\omega_o^{d_s}b^{2d_f/d_l}}k^{2-d_f-2d_f/d_l}(\bar{A}t)^{-\mu}\right) . \qquad \text{(C22)}$$

Assuming $R_g \gg b$ we have $Bt^\nu \gg (k_B T/\eta R_g)t$ in the relevant time regime $t \ll \tau_N$. In this case we find, to leading order, a pure stretched exponential decay,

$$S_p(k,t) \approx \exp\left(-\frac{1}{6}k^2 B t^\nu\right) \approx \exp\left[-(\Gamma_k t)^\nu\right] . \qquad \text{(C23)}$$

---

[1] R. Elber and M. Karplus, Phys. Rev. Lett. **56**, 394 (1986).

[2] M.B. Enright and D.M. Leitner, Phys. Rev. E **71**, 011912 (2005).

[3] X. Yu and D.M. Leitner, J. Chem. Phys. **119**, 12673 (2003); D.M. Leitner, Annu. Rev. Phys. Chem. **59**, 233(2008).

[4] R. Burioni, D. Cassi, F. Cecconi, and A. Vulpiani, Proteins: Struct Func Bioinf **55**, 529 (2004); R. Burioni, D. Cassi, M. P. Fontana, and A. Vulpiani, Europhys. Lett. **58**, 806 (2002).

[5] R. Granek and J. Klafter, Phys. Rev. Lett. 95, 098106 (2005).

[6] S. Reuveni, R. Granek, and J. Klafter, Phys. Rev. Lett. **100**, 208101 (2008).

[7] M. de Leeuw, S. Reuveni, J. Klafter, and R. Granek, PLoS ONE **4**, e7296 (2009).

[8] S. Reuveni, R. Granek, and J. Klafter, Proc. Natl. Acad. Sci. **107**, 13696 (2010).

[9] A. Banerji, I. Ghosh, PLoS ONE **4**, e7361 (2009).

[10] R. Granek, Phys. Rev. E **83**, 020902(R) (2011).

[11] H. J. Stapleton, J. P. Allen, C. P. Flynn, D. G. Stinson, and S. R. Kurtz, Phys. Rev. Lett. **45**, 1456 (1980).

[12] S. G. Lushnikov, A. V. Svanidze, and I. L. Sashin, JETP Letters **82**, 30 (2005).

[13] For a review, see: A. Banerji and I. Ghosh, Cell. Mol. Life Sci. **68**, 2711 (2011).

[14] S.C. Kou and X.S. Xie, Phys. Rev. Lett. **93**, 180603, (2004); W. Min, G. Luo, B. J. Cherayil, S. C. Kou, and X. S. Xie, *ibid.* **94**, 198302 (2005).

[15] P. Senet, G. G. Maisuradze, C. Foulie, P. Delarue, and H. A. Scheraga, Proc. Natl. Acad. Sci. **105**, 19708 (2008).

[16] T. Neusius, I. Daidone, I. M. Sokolov, and J. C. Smith, Phys. Rev. Lett. **100**, 188103 (2008).

[17] M. T. Zimmermann, A. Skliros, A, Kloczkowski, and R. L. Jernigan, Immunome Research 7:5 (2011); http://www.immunome-research.net/xxx.

[18] D. Stauffer and A. Aharony, *Introduction to percolation theory*, Second Edition (Taylor & Francis, London, 1992).

[19] For a review, see: T. Nakayama, K. Yakubo, and R. L. Orbach, Rev. Mod. Phys. **66**, 381 (1994).

[20] S. Alexander and R. Orbach, J. Physique Lett. **43**, L625 (1982).

[21] S. Alexander, Phys. Rev. B **40**, 7953 (1989).

[22] H. Morita and M. Takano, Phys. Rev. E **79**, 020901(R) (2009).

[23] I. Bahar, A. R. Atilgan, and B. Erman, Fold. Des. **2**, 173 (1997); I. Bahar, A. R. Atilgan, M. C. Demirel, and B. Erman, Phys. Rev. Lett. **80**, 2733 (1998).

[24] M.E. Cates, J. Phys. (France) **46**, 1059 (1985).

[25] M. Monkenbusch and D. Richter, C. R. Physique **8**, 845 (2007).

[26] M. Monkenbusch, D. Richter and R. Biehl, ChemPhysChem **8**, 1188 (2010).

[27] J. Lal, P. Fouquet, M. Maccarini, and L.Makowski, J. Mol. Biol. **397**, 423 (2010).

[28] J. H. Roh, J. E. Curtis, S. Azzam, V. N. Novikov, I. Peral, Z. Chowdhuri, R.B. Gregory, and A.P. Sokolov, Biophys. J. **91**, 2573 (2006).

[29] S. Khodadadi, S. Pawlus, J. H. Roh, V. Garcia Sakai, E. Mamontov, and A. P. Sokolov, J. Chem. Phys. **128**, 195106 (2008).

[30] L. Hong, N. Smolin, B. Lindner, A. P. Sokolov and J. C. Smith, Phys. Rev. Lett. **107**, 148102 (2011).

[31] G. R. Kneller and K. Hinsen,J .Chem. Phys., **121**, 10278 (2004).

[32] V. Calandrini, V. Hamon, K. Hinsen, P. Calligari, M.-C. Bellissent-Funel and G.R. Kneller, Chem. Phys. **345**, 289 (2008).

[33] M. Doi and S.F. Edwards, *The Theory of Polymer Dynamics* (Clarendon, Oxford, 1986).

[34] A.G. Zilman and R. Granek, Phys. Rev. E **58**, R2725 (1998).

[35] A. Blumen, Ch. von Ferber, A. Jurjiu, and Th. Koslowski, Macromolecules **37**, 638 (2004); A. Blumen, A. Jurjiu, Th. Koslowski, and Ch. von Ferber, Phys. Rev. E **67**, 061103 (2003).

[36] A. Bunde, H. E. Roman, S. Russ, A. Aharony, and A. B. Harris, Phys. Rev. Lett. **69**, 3189 (1992).

[37] J.W. Kantelhardt and A. Bunde, Phys. Rev. E **56**, 6693 (1997).

[38] S. Reuveni, R. Granek, and J. Klafter, Phys. Rev. E **81**, 040103(R) (2010).

[39] S. Reuveni, R. Granek, and J. Klafter, Phys. Rev. E **82**, 041132 (2010).

[40] L.-W. Yang, E. Eyal, C. Chennubhotla, J. JunGoo, A. M. Gronenborn, and I. Bahar, Structure **15**, 741 (2007).

[41] B. J. Berne and R. Pecora, *Dynamic Light Scattering*, (Wiley, Malabar, 1990).

[42] T. Takedaa, Y. Kawabata, H. Seto, S. Komura, S.K. Ghosh, M. Nagao, and D. Okuhara, J. of Physics and Chemistry of Solids **60**, 1375 (1999); S. Komura, T. Takeda, H. Seto, and M. Nagao in *Neutron Spin Echo Spectroscopy: Basics, Trends and Applications*, F. Mezei, C. Pappas, and T. Gutberlet *eds.* (Springer, Berlin, 2003).

[43] P. Falus, M. A. Borthwick, and S. G. J. Mochrie, Phys. Rev. Lett. **94**, 016105 (2005); P. Falus, M. A. Borthwick, S. Narayanan, A. R. Sandy, and S. G. J. Mochrie, Phys. Rev. Lett. **97**, 066102 (2006).

[44] The hydrodynamic radius may be estimated using the Kirkwood-Riseman formula [33, 45] $R_h^{-1} = \langle R_{ij}^{-1} \rangle$ where $R_{ij} = |\vec{R}_i - \vec{R}_j|$.

[45] W. Van Saarloos, Physica **147A**, 280 (1987); M. Lattuada, H. Wu, and M. Morbidelli, J. Colloid and Interface Sci. **268**, 96 (2003).

[46] H. M. Lindsay, R. Klein, D. A. Weitz, M. Y. Lin, and P. Meakin, Phys. Rev. A **38**, 2614 (1988).

[47] N. G. Van Kampen, *Stochastic Processes in Physics and Chemistry* (North-Holland, Amsterdam, 1992).

[48] G. Stokes, Trans. Cambridge Philos. Soc. **9**, 5 (1856); A. Einstein, Ann. Physik (Leipzig) **19**, 371 (1906); P. Debye, *Polar molecules* (Dover, New York, 1929).

[49] P. M. Chaikin and T. C. Lubensky, *Principles of Condensed Matter Physics* (Cambridge Uni. Press, Cambridge, 1995).

[50] P.-G. de Gennes, *Scaling Concepts in Polymer Physics* (Cornell Uni. Press, Ithaca, 1988).

[51] For a dataset of d_s and d_f values containing about 5,000 proteins see the supporting information in Ref. [7].

[52] A.H. Krall and D.A. Weitz, Phys. Rev. Lett. **80**, 778 (1998).

[53] E. L. Aiden, N. L. van Berkum, L. Williams, M. Imakaev, T. Ragoczy, A. Telling, I. Amit, B. R. Lajoie, P. J. Sabo, M. O. Dorschner, R. Sandstrom, B. Bernstein, M. A. Bender, M. Groudine, A. Gnirke, J. Stamatoyannopoulos, L. A. Mirny, E. S. Lander and J. Dekker, Science **326**, 289 (2009); A. Y. Grosberg, S. K. Nechaev, and E. I. Shakhnovich, J. Physique (France) **49**, 2095 (1988); A. Y. Grosberg, Y. Rabin, S. Havlin, and A. Neer, Europhys. Lett. **23**, 373 (1993); J. G. McNally and D. Mazza, The EMBO Journal **29**, 2 (2010); A. J. Einstein, H.-S. Wu, M. Sanchez, and J. Gil, J. Pathol. **185**, 366 (1998); V. Bedin, R. L. Adam, B. C. S. de Sá, G. Landman, and K. Metze, BMC Cancer **10**, 260 (2010).

[54] J. Mattsson, H. M. Wyss, A. Fernandez-Nieves, K. Miyazaki, Z. Hu, D. R. Reichman, and D. A. Weitz, Nature **462**, 83 (2009).

[55] A.M. Klibanov, Science, **219**, 722 (1983).

[56] E. K. Katzir, Trends Biotechnol. **11**, 471 (1993).

[57] M. Tehei, J.C. Smith, C. Monk, J. Ollivier, M. Oettl, V. Kurkal, J.L. Finney and R.M. Daniel, Biophys. J., **90**, 1090 (2006).
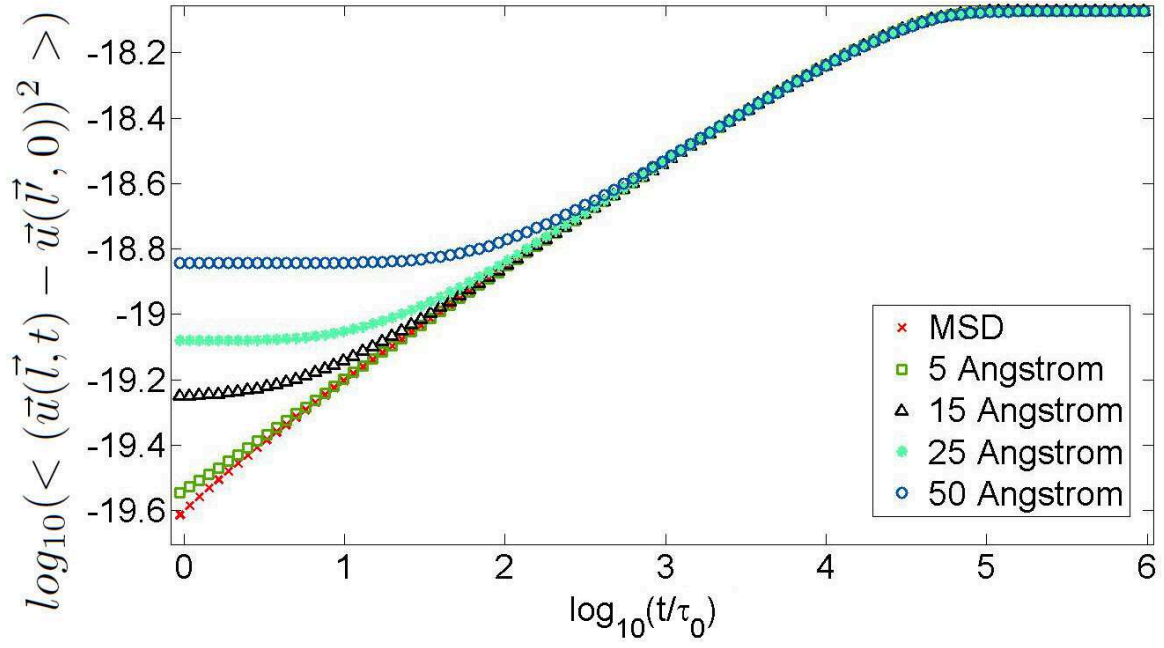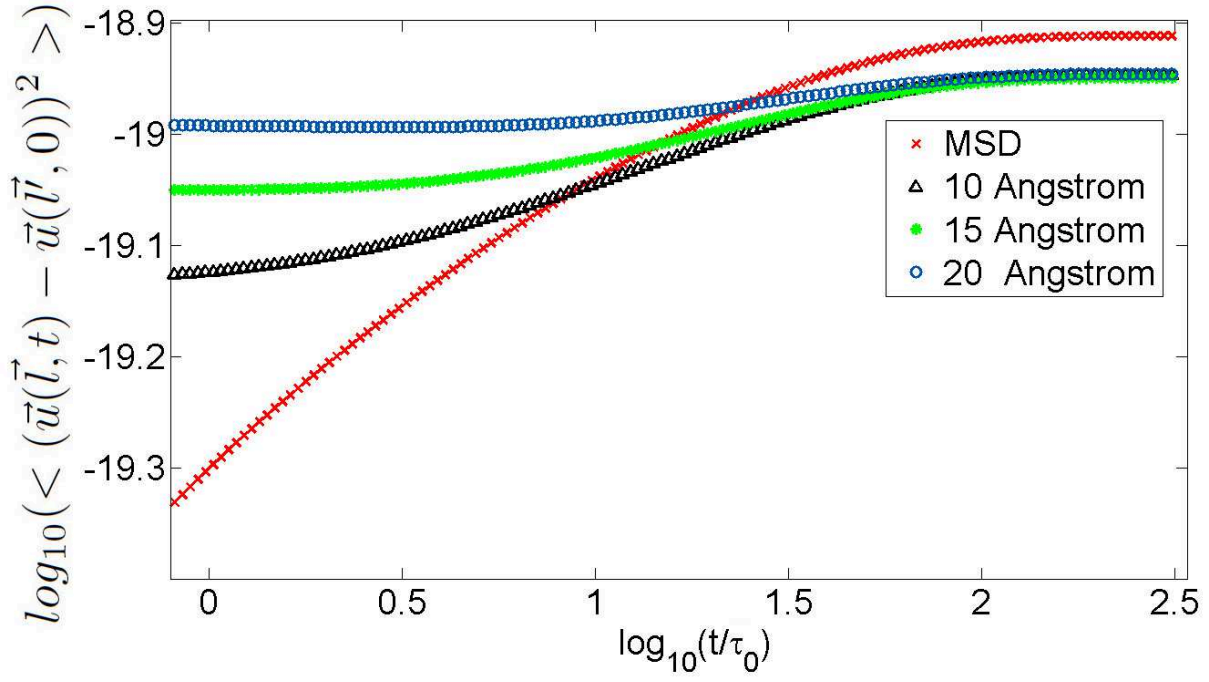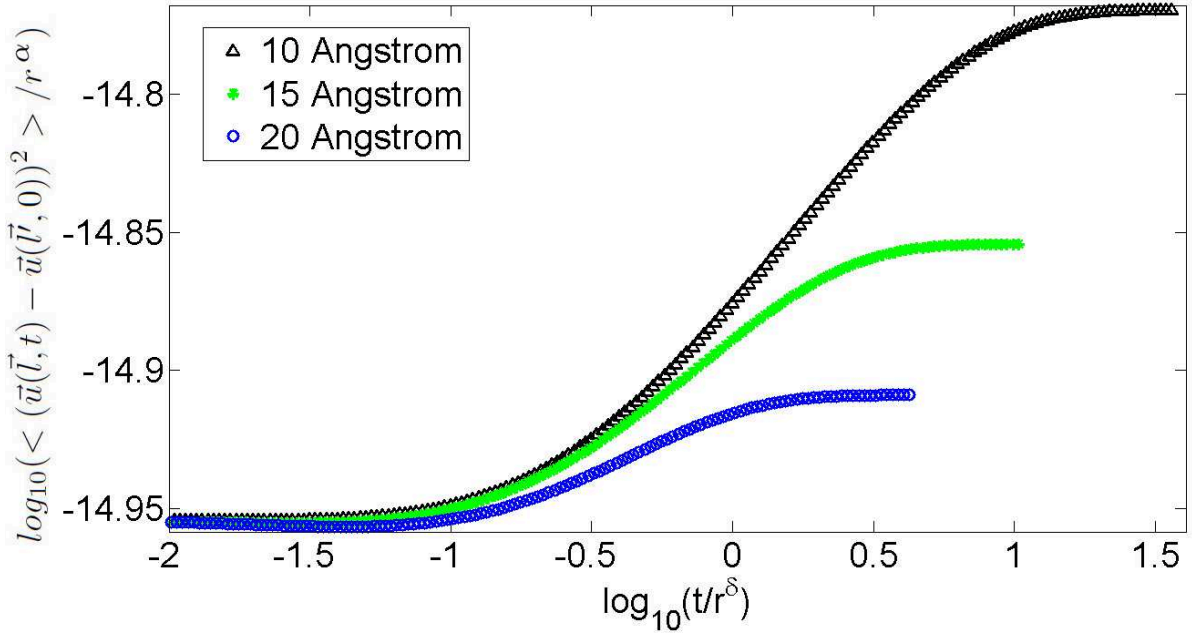
(a)
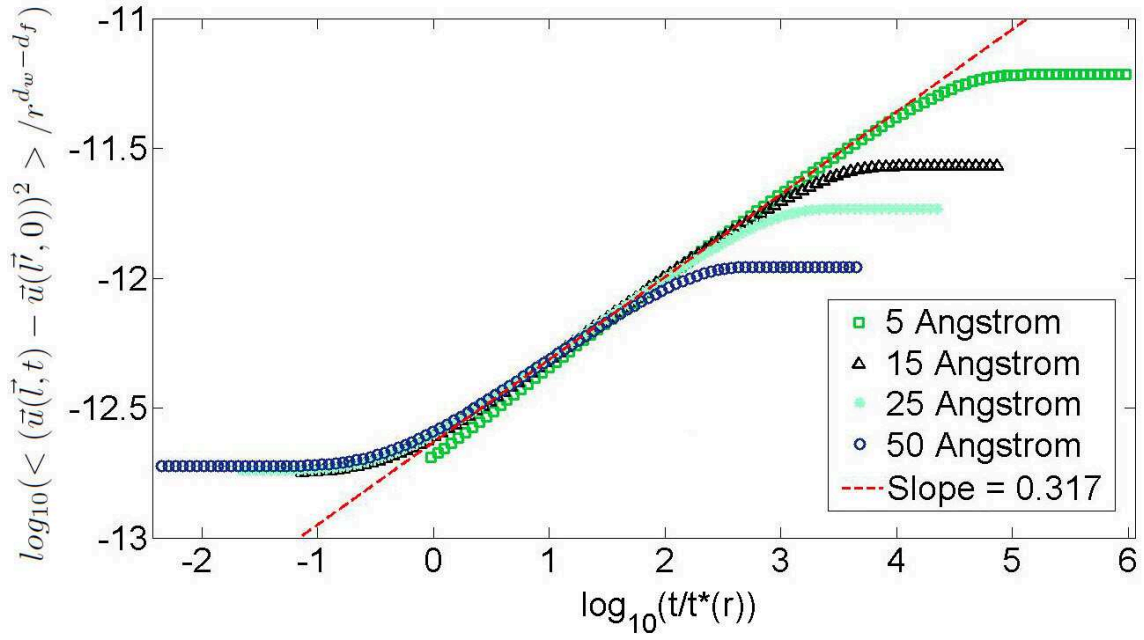
(b)

FIG. 1: **(a) Two point correlation function for the Sierpinski gasket.** The pair correlation function $< (\vec{u}(\vec{l}, t) - \vec{u}(\vec{l'}, 0))^2 >$ is evaluated numerically for bead pairs located on a vibrating Sierpinski gasket with 6561 nodes. Here, we focus on four groups of bead pairs, distanced $r = 5, 15, 25, 50 \pm \frac{1}{2}A$ apart correspondingly. For a *fixed* value of the inter-bead distance r, $< (\vec{u}(\vec{l}, t) - \vec{u}(\vec{l'}, 0))^2 >$ is calculated for all pairs distanced $r \pm \frac{1}{2}A$ apart. For every point in time, the correlation functions, in each distance group, are averaged over all pairs in that group. We plot the averaged two-point correlation functions *vs.* the normalized time t/τ_0, on a log-log scale. Note the crossover from a constant value, that increases with increasing r as predicted by Eq. (52), to an anomalous subdiffusion time regime, identical to that of the single particle MSD (plotted for comparison). As implied by Eq. (51), the crossover time to the anomalous subdiffusion regime, increases with r. In the subdiffusion regime, the correlation function obeys equation (53). As the second term in equation (53) is only a small correction, behavior is expected to not depend on the inter-bead distance. Indeed, a common power law behavior is observed for all distance groups. For long times, all curves saturate to a fixed value equal to $2 < u^2 >_T$, i.e. twice the static MSD.

(b) Scaled plot of (a). Following the predicted scaling behavior stated in Eq. (56), we normalize the correlation functions from (a) by $r^{d_w - d_f}$ and the time by $t^*(r) \sim r^{d_w}$. Data collapse to a single master curve is observed for $\tau_0 \ll t \ll \tau_N$. The slope ν in the subdiffive time regeim is found to be 0.317, in excelet agrrement with the theoretical, Rouse model, value of $\nu = 1 - \frac{d_s}{2} \simeq 0.317$.

(a)

(b)

FIG. 2: **(a) Two point correlation function for the protein LysX, PDB code 1UC8,** $N = 505$**.** The pair correlation function $< (\vec{u}(\vec{l}, t) - \vec{u}(\vec{l'}, 0))^2 >$ is evaluated numerically for amino acids pairs in a procedure identical to the one used for the Sierpinski gasket. We plot, on a log-log scale, the averaged two-point correlation functions *vs.* the the normalized time t/τ_0, for $r = 10, 15, 20 A$. Note again the crossover from a constant value, that increases with r as predicted by Eq. (52), to an effective anomalous subdiffusion time regime. As implied by Eq. (51), the crossover time increases with r. Unlike the Sierpinski gasket, finite size effects are clearly discernible. Curves do not saturate to the exact same value, showing that the average of $< u^2 >_T$ over a given subset of amino acids may not be identical to the average over a different subset, and may also differ from the complete spacial average. In addition, a clear subdiffusion regime is apparent only for the MSD.

(b) Scaled plot of (a). Similar to Fig. 1(a) we normalize the correlation functions from (a) by r^α and the time by r^δ. As finite size effects may modify exponents [8], we allow α and δ to deviate from $d_w - d_f$ and d_w respectively, and search for exponents that collapse the data into a single master curve in the time regime $\tau_0 \ll t \ll \tau_N$). We find that the values $\alpha = 0.464$ and $\delta = 3.09$ best collapse the data, these values are not too far from the predicted values $\alpha = 0.392$ and $\delta = 2.9$.
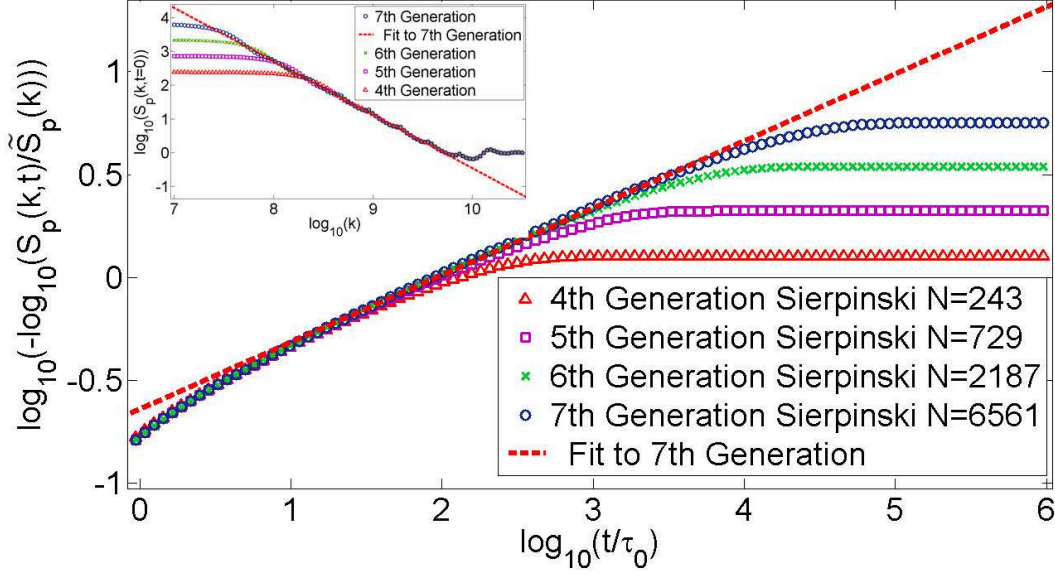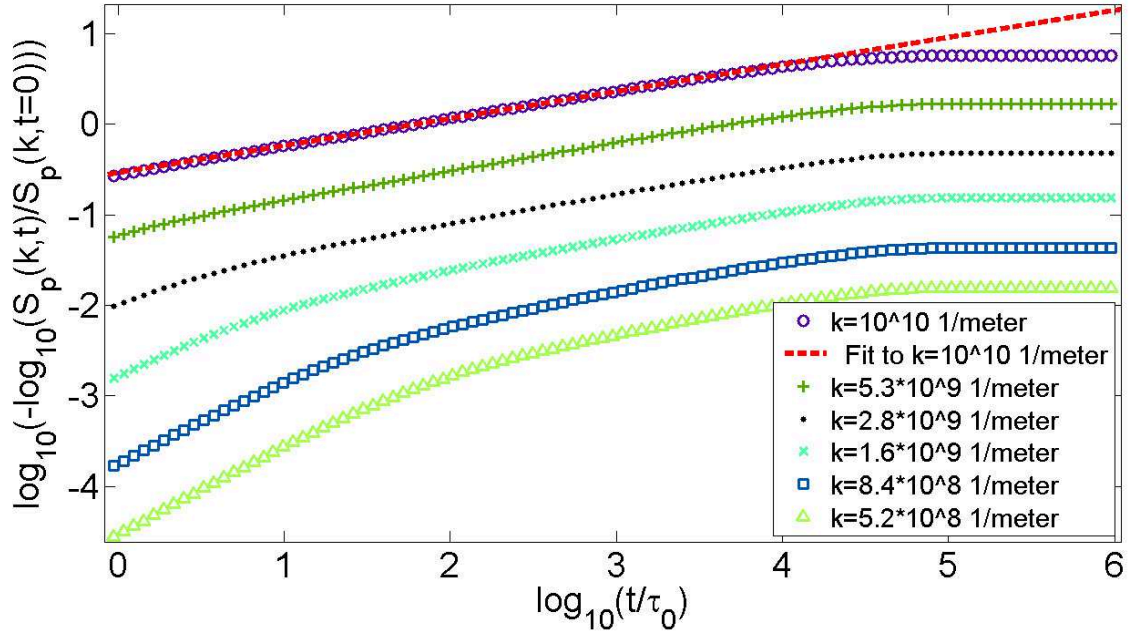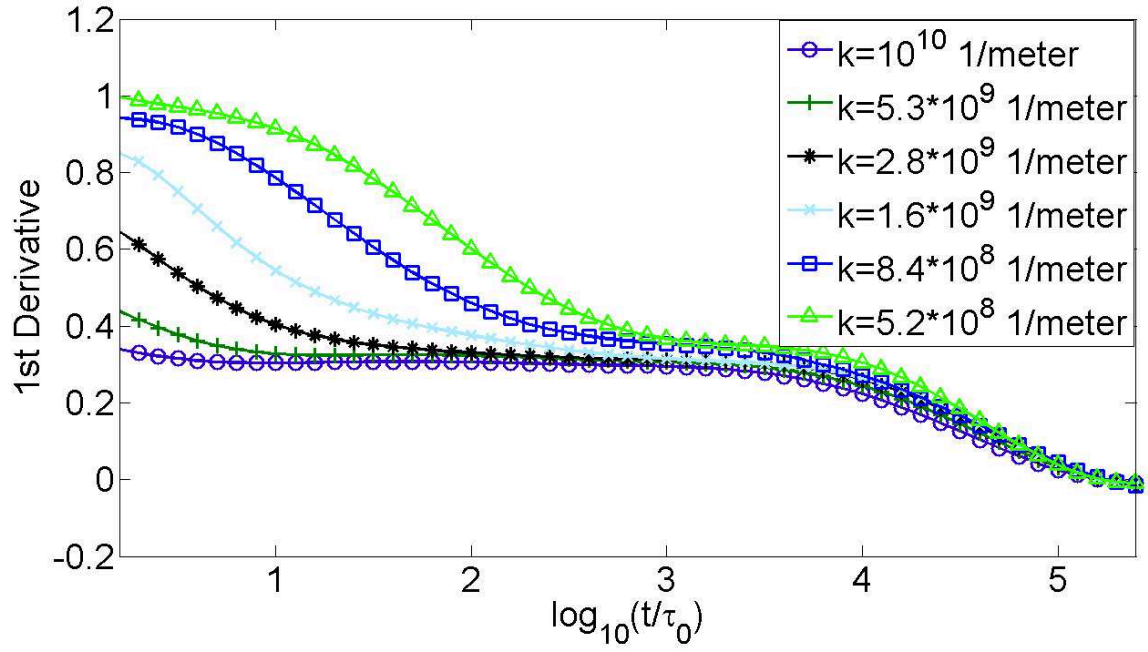
FIG. 3: **Dynamic structure factor of Sierpinski gaskets of various sizes.** In order to demonstrate the stretched exponential decay of the dynamic structure factor for fractal objects we plot $\log_{10}\left[-\log_{10}\left[S(k,t)/\tilde{S}(k)\right]\right]$ *vs.* $\log_{10}(t/\tau_0)$ for Sierpinski gaskets of various sizes. Here $\tilde{S}(k)$ is the frozen structure factor, $k = 10^{10}\mathrm{m}^{-1}$, $\tau_0 = 10.53\mathrm{ps}$ and t ranges from 10ps and up to $10\mu s$. A clear stretched exponential decay, the onset of which starts at $t \simeq 10\tau_0$, is visible for all gaskets. As expected, the time regime into which this decay extends is shown to grow with the size of the gasket. For the largest gasket (7th generation, $N = 6561$, $R_g = 42.6\mathrm{nm}$), the stretched exponential decay persists for approximately three decades. Fitting the data for this gasket, in the time interval $\log_{10}(t/\tau_0) \in (0.81, 3.9)$, we find an exponent of $\simeq 0.325$, with excellent agreement with the theoretical value of $1 - \frac{d_s}{2} \simeq 0.317$.

Inset: The static structure factor of the Sierpinski gasket We plot $S(k, t = 0)$ *vs.* the wave number k on a log-log scale. Here k ranges from $10^7\mathrm{m}^{-1}$ and up to $3.16 \times 10^{10}\mathrm{m}^{-1}$. A clear power law decay, terminating at roughly $k \simeq 10^{9.5}\mathrm{m}^{-1}$, is visible for all gaskets. As expected, the wave number regime in which this decay is observed is shown to grow with the size of the gasket. For the largest gasket the power law decay persists for about two decades. Fitting the data for this gasket, in the wave number interval $\log_{10}(k) \in (7.8, 9.5)$, we find an exponent of -1.583. This value stands in excellent agreement with the theoretical value of $d_f \simeq 1.585$. We note that in contrast to the frozen structure factor $\tilde{S}(k)$, the static structure factor $S(k, t = 0)$ does take into account the contribution of thermal vibrations (see main text). However, as is evident from the plot, vibrations have a negligible effect on the static structure factor for realistic spring constants and temperatures.

(a)

(b)

FIG. 4:

(a) Dynamic structure factor of the Sierpinski gasket – wavenumber dependence. In order to demonstrate the dependence of the stretched exponential decay upon the wave number k we plot $\log_{10}[-\log_{10}[S(k,t)/S(k,t=0)]]$ *vs.* $\log_{10}(t/\tau_0)$ for various values of k. Here $S(k,t=0)$ is the static structure factor, $\tau_0 = 10.53$ps and t ranges from 10ps and up to 10μs. All data is plotted for the 7th generation Sierpinski gasket ($N = 6561$, $R_g = 42.6$nm). As expected, as the wave number k decreases, the onset of the stretched exponential decay (roughly proportional to $\tau(k) \sim k^{-d_f\theta/d_s}$) is pushed towards later times. For $k = 10^{10}$m^{-1} we fit the data in the time interval $\log_{10}(t/\tau_0) \in (0.81, 3.9)$ and find an exponent of 0.30, in excellent agreement with the theoretical value of $1 - \frac{d_s}{2} \simeq 0.317$. Note that in this figure we have used $S(k,t=0)$ as a normalizing factor for $S(k,t)$. This is done in order to verity the quality of the stretched exponential behavior when such an experimental-type analysis of the data is being performed, since $\tilde{S}(k)$ is not a measurable quantity, unlike $S(k)$.

(b) Local slope analysis of the data plotted in (a). The first derivative of $\log_{10}[-\log_{10}[S(k,t)/S(k)]]$, with respect to $\log_{10}[t/\tau_0]$, is plotted *vs.* $\log_{10}[t/\tau_0]$. A clear plateau ("shoulder") region is formed on an intermediate time window that widens up as k increases. For the smallest k studied, this region is visible for $\log_{10}[t/\tau_0] \in (3, 3.75)$ and for the largest k studied it extends across $\log_{10}[t/\tau_0] \in (0.5, 3.75)$. The height of the plateau region corresponds to the value of the exponent which characterizes the stretched exponential decay. As k increases, the height of the plateau region slowly converges to a value of $\simeq 0.30$, remarkably close the theoretical value $\beta = \nu = 1 - d_s/2 \simeq 0.317$
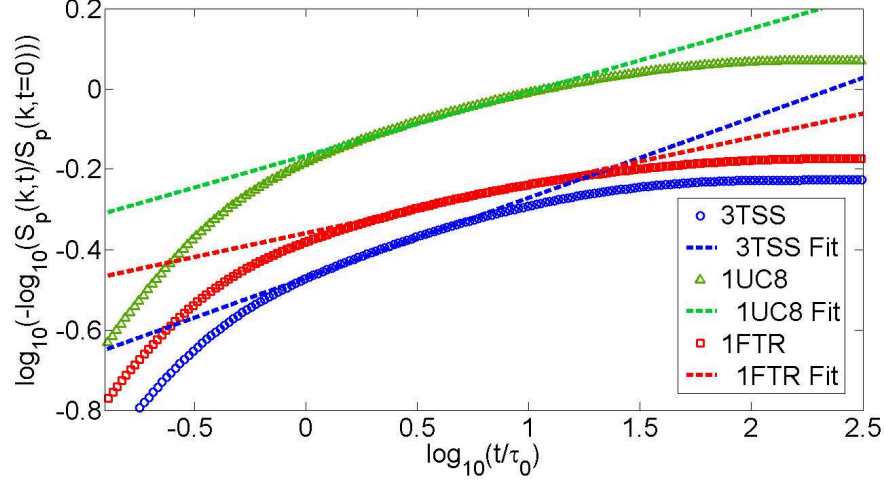
(a)
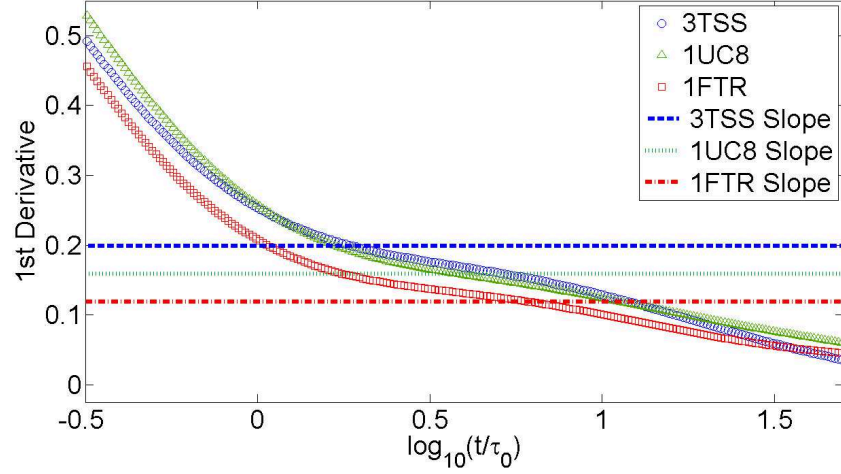
(b)

FIG. 5: **(a) Dynamic structure factor of proteins.** $-\log_{10}[S_p(k,t)/S_p(k)]$ *vs.* t/τ_0 is plotted on a log-log scale for three different proteins, 1FTR ($N = 1184$), 1UC8 ($N = 505$), and 3TSS ($N = 190$). Here $\tau_0 = \gamma/\omega_o^2 = 22.19, 32.29, 16.78$ps respectively and $k = 10^{10}$m^{-1}. As in Fig. 4a, we divide the dynamic structure factor by the static structure factor $S_p(k) \equiv S(k, t = 0)$. The decay is clearly non-exponential. However, unlike Fig. 4a we do not observe a clear straight line in an intermediate time window that spans across several time decades, indicating that the decay is not a pure stretched exponential. The effective stretching exponents that are obtained in an approximate fit are $\beta = 0.119, 0.1584, 0.199$, respectively. **(b) Local slope analysis of the data plotted in (a).** The first derivative of $\log_{10}[-\log_{10}[S(k,t)/S(k)]]$, with respect to $\log_{10}[t/\tau_0]$, is plotted *vs.* $\log_{10}[t/\tau_0]$. The horizontal dashed lines are the slope values obtained from the fits in (a). It can be seen that these lines cross the derivative lines in the middle of a weak "shoulder" that signifies an approximate stretched exponential regime.
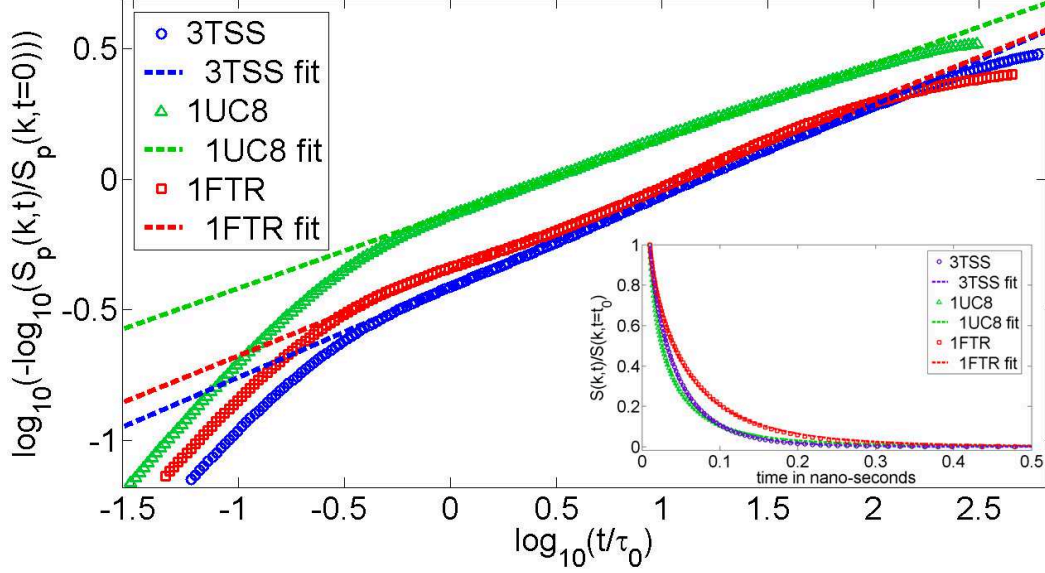
48

FIG. 6: **The joint effect of vibrations and rotations on the dynamic structure factor of proteins.** Numerically evaluating $S_p(k,t)$, Eq. (68) (or Eq. (B11)), we study the joint effect of vibrations and rotations on the dynamic structure factor. We plot $-\log_{10}[S_p(k,t)/S_p(k)]$ *vs.* t/τ_0 on a log-log scale for the same three proteins that appear in figure 5. We observe a clear, effective, stretched exponential decay of the dynamic structure factor in an intermediate time regime. The effective stretching exponents are $\beta = 0.34, 0.28, 0.32$ for 3TSS, 1UC8 and 1FTR respectively. Note that these exponents are higher than the ones obtained when only vibrations were taken into account. **Inset: The contribution of translations.** Numerically evaluating $S(k,t)$, Eq. (63), we add the contribution of translations to that of vibrations and rotations. We now follow Ref. [27], define $t_0 = 0.01ns$, and plot $S(k,t)/S(k,t_0)$ vs. the time in nano-seconds. The cumulative effect of all three terms give rise to a non-exponential decay that can be well fitted by a stretched exponential in the time interval $t \in [0.01ns, 1ns]$. The effective stretching exponents are $\beta = 0.72, 0.42, 0.65$ for 3TSS, 1UC8 and 1FTR respectively. Note again that, as expected, these exponents are higher than the ones obtained when only vibrations and rotations are taken into account. Since the decay due to translations is purely exponential, we conclude that the origins of the apparent stretched exponential are the contributions due to vibrations and rotations. However, the exact value of the effective stretching exponent is sensitive to the interplay between vibrations, rotations and translations. It is therefore non-universal and may vary from protein to protein and with external conditions.

49